Secure and Energy-Efficient Beamforming for Simultaneous Information and Energy Transfer

Ali Arshad Nasir, *Member, IEEE*, Hoang Duong Tuan, Trung Q. Duong, *Senior Member, IEEE*, and H. Vincent Poor, *Fellow, IEEE*

***Abstract*— Some next-generation wireless networks will likely involve the energy-efficient transfer of information and energy over the same wireless channel. Moreover, densification of such networks will make the physical layer more vulnerable to cyber attacks by potential multi-antenna eavesdroppers. To address these issues, this paper considers transmit time-switching (TS) mode, in which energy and information signals are transmitted separately in time by the base station (BS). This protocol is not only easy to implement but also delivers the opportunity for multi-purpose beamforming, in which energy beamformers can be used to jam eavesdroppers during wireless power transfer. In the presence of imperfect channel estimation and multi-antenna eavesdroppers, the energy and information beamformers and the transmit TS ratio are jointly optimized to maximize the worst-case user secrecy rate subject to energy constrained users' harvested energy thresholds and a BS transmit power budget. New robust path-following algorithms, which involve one simple convex quadratic program at each iteration are proposed for computational solutions of this difficult optimization problem and also the problem of secure energy efficiency maximization. The latter adds further complexity due to additional optimization variables appearing in the denominator of the secrecy rate function. Numerical results confirm that the performance of the proposed computational solutions is robust against channel uncertainties.**

***Index Terms*— Secrecy rate, secrecy energy efficiency, wireless power transfer, time switching, beamforming, nonconvex programming.**

Manuscript received January 1, 2017; revised April 1, 2017 and July 2, 2017; accepted September 1, 2017. Date of publication September 12, 2017; date of current version November 9, 2017. This work was supported in part by the King Fahd University of Petroleum and Minerals under a Start-up Research Project #SR161003, in part by the Australian Research Council's Discovery Projects under Project DP130104617, in part by a U.K. Royal Academy of Engineering Research Fellowship under Grant RF1415/14/22, in part by the U.K. Engineering and Physical Sciences Research Council under Grant EP/P019374/1, and in part by the U.S. National Science Foundation under Grant CNS-1702808 and Grant ECCS-1647198. This paper was presented in part at the IEEE GLOBECOM Workshop on Trusted Communications with Physical Layer Security, Singapore, December, 2017. The associate editor coordinating the review of this paper and approving it for publication was B. Clerckx. *(Corresponding author: Trung Q. Duong.)*

A. A. Nasir is with the Department of Electrical Engineering, King Fahd University of Petroleum and Minerals, Dhahran, Saudi Arabia (e-mail: anasir@kfupm.edu.sa).

H. D. Tuan is with the School of Electrical and Data Engineering, University of Technology Sydney, Broadway, NSW 2007, Australia (e-mail: tuan.hoang@uts.edu.au).

T. Q. Duong is with Queen's University Belfast, Belfast BT7 1NN, U.K. (e-mail: trung.q.duong@qub.ac.uk).

H. V. Poor is with the Department of Electrical Engineering, Princeton University, Princeton, NJ 08544 USA (e-mail: poor@princeton.edu).

Color versions of one or more of the figures in this paper are available online at http://ieeexplore.ieee.org.

Digital Object Identifier 10.1109/TWC.2017.2749568

I. Introduction

NEXT-GENERATION communication networks offer the potential to transfer information and energy through the same wireless communication channel, where energy constrained users (UEs) would be able to not only receive information but also harvest energy [1]–[3]. The information transfer generally aims at high signal-to-interference-plus-noise-ratio (SINR) while the energy transfer aims at a high-power ambient signal [4], [5]. Early work in this area considered systems in which information and energy are transferred simultaneously by the same signals. To realize both wireless energy harvesting (EH) and information decoding (ID) in such systems, UE receivers need to split the received signal for EH and ID either by power splitting (PS) or time switching (TS) [6], [7]. Our recent work in [8] shows that such protocols, particularly the PS approach at the receiver, is not only complicated and inefficient for practical implementation, but also not necessary. It is much more efficient to transfer information and energy separately, in which case the UE receiver does not need any sophisticated hardware for this purpose.

Wireless power transfer is more viable in sensor networks or in dense small-cell deployments where there is closer proximity between the base station (BS) and UEs. Such densification of wireless networks makes the wireless devices more vulnerable to eavesdropping than in sparser networks [9], [10]. Physical layer security aims to secure data transmissions in such networks [11]–[13]. Several recent works have considered the problem of designing a beamformer to maximize secrecy rate under a BS transmit power budget [14]–[17]. Beamforming requires the knowledge of downlink channels to the UEs, which can be obtained via channel estimation. Due to channel estimation errors in practical systems, the BS cannot expect perfect channel knowledge, which thus necessitates the design of beamformers that are robust to channel uncertainties [14], [16]. Adding EH introduces an additional constraint in the secrecy rate optimization problem [18].

Robust beamformer design in the presence of channel uncertainties with the same objective of secrecy rate maximization under receiver EH thresholds in addition to a BS transmit power budget has recently been considered in [19]–[22]. Some of these works assume either only EH or only ID capability at the UEs [20], [21], so they did not consider PS or TS based simultaneous wireless information and power transfer (SWIPT) receivers. Assuming PS-based SWIPT receivers, secrecy rate maximization was studied in [19] and

[22]. These works employ semi-definite programming and alternating optimization, in which rank-one constraints have to be dropped and computationally complex matrices have to be optimized. Randomization has to be employed to achieve feasible beamforming vectors [22]. As has been pointed out in [23], such a randomization approach is inefficient. Moreover, it is not easy to implement the variable range power splitter needed for PS, and further, jamming the eavesdropper requires transmitting artificial noise [8]. In contrast, as shown in the current paper, our recently proposed transmit TS approach [8] does not require transmission of extra artificial noise thanks to the fact that power-bearing signals sent during EH periods can be simultaneously used to jam the eavesdropper.

Meanwhile, optimization of energy efficiency (EE) in terms of bits per Joule per Hertz is also a very important issue in the design of emerging communication networks (see e.g. [24]–[29]), where the Dinkelbach-type algorithm [30] of fractional programming is the main tool for obtaining computational solutions (see e.g. [31], [32] and references therein). In the presence of eavesdroppers, secrecy energy efficiency (SEE) maximization has been studied recently in [33] and [34]. However, the approach proposed to treat SEE in [33] and [34] is based on costly beamformers, which completely cancel the multi-user interference and signals received at the eavesdroppers. The introduction of energy harvesting introduces conflicting requirements from the viewpoint of EE, as it requires a stronger transmit power. The problem of energy efficiency maximization in SWIPT systems has been recently studied in [35]–[37]. However, either the authors do not consider simultaneous EH and ID capability [37] or they assume PS based receivers [35], [36]. To the best of our knowledge, robust beamforming design to achieve secrecy rate and SEE optimization, particularly assuming practical TS-based wireless EH systems, has not been considered previously.

The subject of this paper is a multicell network, in which the UEs in each cell are divided into two groups depending upon their distance from the serving BS. Those closer to the BS take advantage of higher received power to perform wireless EH in addition to ID while the far-away users only conduct ID. We consider the situation in which the BSs have imperfect knowledge about the channels to UEs and eavesdroppers. We consider the transmit TS approach [8] in which the BS transmits information and energy separately in different time periods and the energy beamformers can be exploited to jam the eavesdroppers. In the presence of channel uncertainties, we formulate a worst-case based robust secrecy rate optimization problem. We consider the joint optimization of information and energy beamforming vectors together with the transmit TS ratio, in order to maximize the minimum secrecy rate among all users, while ensuring EH constraints for near-by users and transmit power constraints at the BSs. This problem is very difficult computationally due to the many challenging constraints, and a path-following algorithm is developed for its solution. The algorithm does not require rank-constrained optimization and converges quite quickly in a few iterations. Through extensive simulation, the achieved secrecy rate is shown to be close to the rate that can be achieved in the absence of eavesdroppers. Furthermore, our numerical results confirm that the performance of the proposed algorithm is close to that attained in the perfect channel knowledge case. In addition, the proposed algorithm not only outperforms the existing algorithm based on power-splitting, but also the proposed transmit TS based system is implementation-wise much simpler than the PS-based system. Finally, we extend our development to solve and analyze the robust SEE maximization problem, which adds further complexity due to the presence of optimization variables in the denominator of the secrecy rate function.

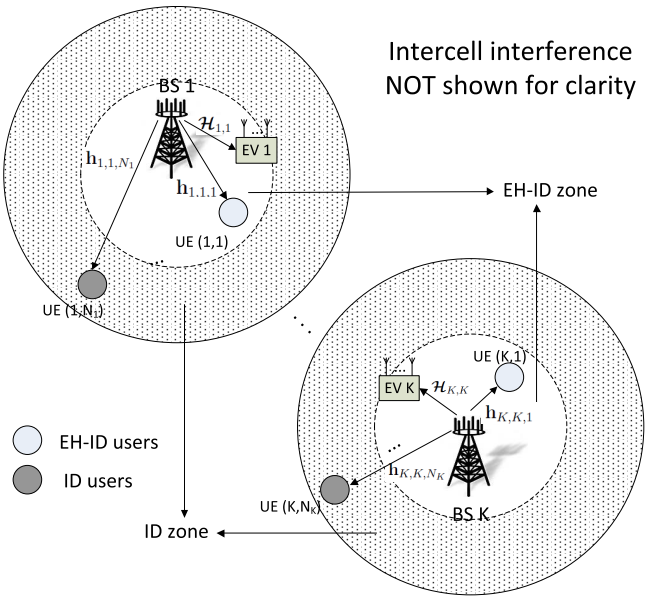

Fig. 1. Downlink multiuser multicell interference scenario in a dense network consisting of K small cells. For clarity, the intercell interference channels are not shown, however, the interference occurs in all K cells.

The paper is organized as follows. Section II presents the problem formulation for maximizing the worst-case user secrecy rate and its challenges, whereas Section III develops its computational solution. Section IV proposes a computational solution for EE maximization. Section V evaluates the performance of our proposed algorithms using numerical examples. Finally, Section VI concludes the paper.

Notation: We use $\Re\{\cdot\}$ to denote the real part of its argument, ∇ to denote the first-order differential operator, and $\|\mathbf{x}\|$ and $\|\mathbf{X}\|_F$ to denote the Euclidean and Frobenius norms of a vector $\mathbf{x}$ and matrix $\mathbf{X}$, respectively. Also, we define $\langle \mathbf{x}, \mathbf{y} \rangle \triangleq \mathbf{x}^H \mathbf{y}$.

II. System Model and Problem Formulation

Consider a multicell network consisting of K small cells labeled by $k \in \mathcal{K} \triangleq \{1, \ldots, K\}$. As shown in Fig. 1, in each cell k, a multi-antenna BS k with M antennas communicates with N_k single-antenna UEs (k, n), $n \in \mathcal{N}_k \triangleq \{1, \ldots, N_k\}$, over the same bandwidth. We divide the users in each cell k into two zones, such that there are $N_{1,k}$ users located nearby serving BS k in zone-1 and $N_{2,k}$ users located far from the BS k in zone-2, where $N_k = N_{1,k} + N_{2,k}$. By UE (k, n_1) and UE (k, n_2), we mean UE $n_1 \in \mathcal{N}_{1,k} \triangleq \{1, \ldots, N_{1,k}\}$ in zone-1 and UE $n_2 \in \mathcal{N}_{2,k} \triangleq \{N_{1,k} + 1, \ldots, N_k\}$ in zone-2 of cell k,

respectively. Moreover, as shown in Fig. 1, we assume that for UEs (k,n) of cell k, there is a single eavesdropper k with N_{ev} antennas in zone-1, who eavesdrops upon the signals intended for UEs (k,n).

BSs intend to transfer energy to only their zone-1 users since they are located sufficiently near to their serving BSs and are able to practically harvest energy. Information is transmitted to both zone-1 and zone-2 users. Denote by $\mathbf{x}^E_{k,n_1} \in \mathbb{C}^{M\times 1}$ and $\mathbf{x}^I_{k,n} \in \mathbb{C}^{M\times 1}$ the EH and ID beamforming vectors used by BS k for its UE (k,n_1) and UE (k,n), respectively. The channel $\widetilde{\mathbf{h}}_{\bar{k},k,n} \in \mathbb{C}^{M\times 1}$ between BS $\bar{k}$ and UE (k,n) is assumed to be frequency flat fading, which incorporates the effects of both large-scale pathloss and small-scale fading. Denote by s^E_{k,n_1} and $s^I_{k,n}$ the respective energy and information signals intended for UE (k,n_1) and UE (k,n) by BS k, with $\mathbb{E}\{|s^E_{k,n_1}|^2\} = \mathbb{E}\{|s^I_{k,n}|^2\} = 1$. Let $0<\eta<1$ be the time splitting for transferring energy and information to UE. The baseband signal received by UE (k,n_1) for EH is

$$y^E_{k,n_1} = \sum_{\bar{k}\in\mathcal{K}} \widetilde{\mathbf{h}}^H_{\bar{k},k,n_1} \sum_{\bar{n}\in\mathcal{N}_{1,\bar{k}}} \mathbf{x}^E_{\bar{k},\bar{n}} s^E_{\bar{k},\bar{n}} + z^a_{k,n_1}, \tag{1}$$

where $z^a_{k,n_1} \sim \mathcal{CN}(0,\sigma_a^2)$ is additive white complex Gaussian noise, with zero-mean and variance σ_a^2, at the receiver of UE (k,n). Using (1) and assuming a linear EH model,[1] the energy harvested by UE (k,n_1) can be written as

$$E_{k,n_1}(\mathbf{x}^E,\eta) \triangleq \zeta_{k,n_1}\eta p_{k,n_1}(\mathbf{x}^E), \tag{2}$$

where

$$p_{k,n_1}(\mathbf{x}^E) \triangleq \sum_{\bar{k}\in\mathcal{K}}\sum_{\bar{n}\in\mathcal{N}_{1,\bar{k}}} |\widetilde{\mathbf{h}}^H_{\bar{k},k,n_1}\mathbf{x}^E_{\bar{k},\bar{n}}|^2 + \sigma_a^2, \tag{3}$$

and $\zeta_{k,n_1} \in (0,1)$ is the energy conversion efficiency for the (k,n_1)-th EH receiver. Here, we assume a common TS ratio η for all BSs, $k \in \mathcal{K}$, where near-by users harvest energy through wireless signals not only from the serving BSs but also from the neighboring BSs. Note that the harvested and stored energy E_{k,n_1} may be used later for different power constrained operations at UE (k,n_1), e.g., assisting uplink data transmission to the BS or performing downlink information processing. Here $\mathbf{x}^E \triangleq [\mathbf{x}^E_{k,n_1}]_{k\in\mathcal{K},n_1\in\mathcal{N}_{1,k}}$. The signal received by UE (k,n) for ID is

$$\begin{aligned} y^I_{k,n} = {} & \widetilde{\mathbf{h}}^H_{k,k,n}\mathbf{x}^I_{k,n}s^I_{k,n} + \widetilde{\mathbf{h}}^H_{k,k,n}\sum_{\bar{n}\in\mathcal{N}_k\setminus\{n\}} \mathbf{x}^I_{k,\bar{n}}s^I_{k,\bar{n}} \\ & + \sum_{\bar{k}\in\mathcal{K}\setminus\{k\}} \widetilde{\mathbf{h}}^H_{\bar{k},k,n}\sum_{\bar{n}\in\mathcal{N}_{\bar{k}}} \mathbf{x}^I_{\bar{k},\bar{n}}s^I_{\bar{k},\bar{n}} + z^a_{k,n}, \end{aligned} \tag{4}$$

where its first term represents the desired signal, while the second and third terms are the intracell interference and intercell interference. The BSs are assumed to perform channel estimation to acquire channel knowledge $\mathbf{h}_{\bar{k},k,n}$ and the channel state information (CSI) errors are bounded by the uncertainty $\epsilon_{\bar{k},k,n}$ as follows [41], [42]:

$$\rho(\widetilde{\mathbf{h}}_{\bar{k},k,n}\widetilde{\mathbf{h}}^H_{\bar{k},k,n} - \mathbf{h}_{\bar{k},k,n}\mathbf{h}^H_{\bar{k},k,n}) \le \epsilon_{\bar{k},k,n}, \tag{5}$$

where $\rho(A)$ is called the spectral radius of matrix A: $\rho(A) = \max_i |\lambda_i(A)|$ with its eigenvalues $\lambda_i(A)$, and the channel uncertainties $\epsilon_{\bar{k},k,n}$ are given by

$$\epsilon_{\bar{k},k,n} = \begin{cases} \epsilon_0\|\mathbf{h}_{\bar{k},k,n}\|^2, & k \ne \bar{k} \\ \epsilon_1\|\mathbf{h}_{\bar{k},k,n}\|^2, & k = \bar{k}, \end{cases} \tag{6}$$

where ϵ_0 and ϵ_1 are the normalized uncertainty levels related to neighboring cells' UEs and the serving cells' UEs, respectively.[2] Note that (5) covers all uncertainty structures [42]. Thus, incorporating the channel uncertainties, the worst-case information rate decoded by UE (k,n) is given by [42]

$$\begin{aligned} & (1-\eta)\log_2(1+\text{SINR-UE}_{k,n}) \\ & \quad \triangleq (1-\eta)\log_2\left(1 + \frac{|\mathbf{h}^H_{k,k,n}\mathbf{x}^I_{k,n}|^2 - \epsilon_{k,k,n}\|\mathbf{x}^I_{k,n}\|^2}{\varphi_{k,n}(\mathbf{x}^I)}\right), \end{aligned} \tag{7}$$

where $\mathbf{x}^I \triangleq [\mathbf{x}^I_{k,n}]_{k\in\mathcal{K},n\in\mathcal{N}_k}$ and

$$\begin{aligned} \varphi_{k,n}(\mathbf{x}^I) \triangleq {} & \underbrace{\sum_{\bar{n}\in\mathcal{N}_k\setminus\{n\}} |\mathbf{h}^H_{k,k,n}\mathbf{x}^I_{k,\bar{n}}|^2}_{\text{intracell interference}} \\ & + \underbrace{\sum_{\bar{k}\in\mathcal{K}\setminus\{k\}}\sum_{\bar{n}\in\mathcal{N}_{\bar{k}}} |\mathbf{h}^H_{\bar{k},k,n}\mathbf{x}^I_{\bar{k},\bar{n}}|^2}_{\text{intercell interference}} \\ & + \sum_{\bar{n}\in\mathcal{N}_k\setminus\{n\}} \epsilon_{k,k,n}\|\mathbf{x}^I_{k,\bar{n}}\|^2 \\ & + \sum_{\bar{k}\in\mathcal{K}\setminus\{k\}}\sum_{\bar{n}\in\mathcal{N}_{\bar{k}}} \epsilon_{\bar{k},k,n}\|\mathbf{x}^I_{\bar{k},\bar{n}}\|^2 + \sigma_a^2. \end{aligned} \tag{8}$$

A multi-antenna eavesdropper with N_{ev} antennas tries to eavesdrop the intended signals for the UE (k,n). The signal received at the EV k is composed of the signal received during time fraction η, denoted by $\mathbf{y}^E_k \in \mathbb{C}^{N_{\text{ev}}\times 1}$ and given by

$$\mathbf{y}^E_k = \sum_{\bar{k}\in\mathcal{K}} \widetilde{\boldsymbol{\mathcal{H}}}^H_{\bar{k},k} \sum_{\bar{n}\in\mathcal{N}_{1,\bar{k}}} \mathbf{x}^E_{\bar{k},\bar{n}}s^E_{\bar{k},\bar{n}} + \mathbf{z}^a_k,$$

and the signal received at the EV k during time fraction $1-\eta$, denoted by $\mathbf{y}^I_k \in \mathbb{C}^{N_{\text{ev}}\times 1}$ given by

$$\mathbf{y}^I_k = \sum_{\bar{k}\in\mathcal{K}} \widetilde{\boldsymbol{\mathcal{H}}}^H_{\bar{k},k} \sum_{\bar{n}\in\mathcal{N}_{\bar{k}}} \mathbf{x}^I_{\bar{k},\bar{n}}s^I_{\bar{k},\bar{n}} + \mathbf{z}^a_k,$$

where $\widetilde{\boldsymbol{\mathcal{H}}}_{\bar{k},k}$ is the wiretap channel matrix of size $M \times N_{\text{ev}}$ between BS $\bar{k}$ and UE k and $\mathbf{z}^a_k \in \mathbb{C}^{N_{ev}}\left(0,\sigma_a^2 I_{N_{\text{ev}}}\right)$ is noise [10], [43]–[45]. Since the eavesdropper is not aware of the time switching factor η, $\mathbf{y}^E_k$ is considered as an additional noise to jam the eavesdropper. Therefore, the noise power at

[1]The recently studied non-linear EH model and waveform design for efficient wireless power transfer [38]–[40] is beyond the scope of this work, but could be incorporated into future research.

[2]We have introduced two different uncertainty levels because later we will show in Section V that secrecy rate is more sensitive to the estimation errors of serving users' channels compared to that of the neighboring users' channels.

EV k in decoding $s^I_{k,n}$ is defined as

$$\eta \sum_{\bar{k}\in\mathcal{K}} \sum_{\bar{n}\in\mathcal{N}_{1,\bar{k}}} \|\widetilde{\boldsymbol{\mathcal{H}}}^H_{\bar{k},k}\mathbf{x}^E_{\bar{k},\bar{n}}\|^2 + (1-\eta)\Big(\sum_{\bar{k}\in\mathcal{K}} \sum_{\bar{n}\in\mathcal{N}_{\bar{k}}} \|\widetilde{\boldsymbol{\mathcal{H}}}^H_{\bar{k},k}\mathbf{x}^I_{\bar{k},\bar{n}}\|^2 - \|\widetilde{\boldsymbol{\mathcal{H}}}^H_{k,k}\mathbf{x}^I_{k,n}\|^2\Big) + N_{\text{ev}}\sigma_a^2. \tag{9}$$

We assume that the wiretap channel state information $\boldsymbol{\mathcal{H}}_{\bar{k},k}$ is available through channel estimation subject to some uncertainty [41], [42]

$$\rho(\widetilde{\boldsymbol{\mathcal{H}}}_{\bar{k},k}\widetilde{\boldsymbol{\mathcal{H}}}^H_{\bar{k},k} - \boldsymbol{\mathcal{H}}_{\bar{k},k}\boldsymbol{\mathcal{H}}^H_{\bar{k},k}) \le \epsilon_{\bar{k},k}, \quad \forall \bar{k},\ k \in \mathcal{K}, \tag{10}$$

where $\epsilon_{\bar{k},k} = \epsilon_0\|\boldsymbol{\mathcal{H}}_{\bar{k},k}\|_F^2$ and ϵ_0 is the normalized uncertainty level for the channels between BSs and the eavesdroppers. Therefore, the worst received SINR at the EV k, corresponding to the signal targeted for the UE (k,n), is given by [42]

$$\text{SINR-EV}_{k,n} \triangleq \frac{\|\boldsymbol{\mathcal{H}}^H_{k,k}\mathbf{x}^I_{k,n}\|^2 + \epsilon_{k,k}\|\mathbf{x}^I_{k,n}\|^2}{q_{k,n}(\mathbf{x},\eta)}. \tag{11}$$

where

$$\begin{aligned} q_{k,n}(\mathbf{x},\eta) &\triangleq \frac{\eta}{(1-\eta)}\left(\sum_{\bar{k}\in\mathcal{K}}\sum_{\bar{n}\in\mathcal{N}_{1,k}} \|\boldsymbol{\mathcal{H}}^H_{\bar{k},k}\mathbf{x}^E_{\bar{k},\bar{n}}\|^2 - \sum_{\bar{k}\in\mathcal{K}}\sum_{\bar{n}\in\mathcal{N}_{1,k}} \epsilon_{\bar{k},k}\|\mathbf{x}^E_{\bar{k},\bar{n}}\|^2\right) \\ &+ \sum_{\bar{n}\in\mathcal{N}_k\setminus\{n\}} \|\boldsymbol{\mathcal{H}}^H_{k,k}\mathbf{x}^I_{k,\bar{n}}\|^2 + \sum_{\bar{k}\in\mathcal{K}\setminus\{k\}}\sum_{\bar{n}\in\mathcal{N}_{\bar{k}}} \|\boldsymbol{\mathcal{H}}^H_{\bar{k},k}\mathbf{x}^I_{\bar{k},\bar{n}}\|^2 \\ &- \left(\sum_{\bar{n}\in\mathcal{N}_k\setminus\{n\}} \epsilon_{k,k}\|\mathbf{x}^I_{k,\bar{n}}\|^2 + \sum_{\bar{k}\in\mathcal{K}\setminus\{k\}}\sum_{\bar{n}\in\mathcal{N}_{\bar{k}}} \epsilon_{\bar{k},k}\|\mathbf{x}^I_{\bar{k},\bar{n}}\|^2\right) \\ &+ N_{\text{ev}}\sigma_a^2/(1-\eta), \end{aligned} \tag{12}$$

where $\mathbf{x} \triangleq [\mathbf{x}^E; \mathbf{x}^I]$.

The main attractive feature in (11)-(12) is that the EH signals contribute very much to the denominator of the SINR (11) at EV k, i.e. they are also used in jamming the EV k. The secrecy rate expression for UE (k,n) in nat/sec/Hz is given as [46]

$$\begin{aligned} f_{k,n}(\mathbf{x},\eta) &= (1-\eta)\ln(1+\text{SINR-UE}_{k,n}) - \ln(1+\text{SINR-EV}_{k,n}) \\ &= (1-\eta)\ln\left(1+\frac{|\mathbf{h}^H_{k,k,n}\mathbf{x}^I_{k,n}|^2 - \epsilon_{k,k,n}\|\mathbf{x}^I_{k,n}\|^2}{\varphi_{k,n}(\mathbf{x}^I)}\right) \\ &\quad - \ln\left(1+\frac{\|\boldsymbol{\mathcal{H}}^H_{k,k}\mathbf{x}^I_{k,n}\|^2 + \epsilon_{k,k}\|\mathbf{x}^I_{k,n}\|^2}{q_{k,n}(\mathbf{x},\eta)}\right) \\ &= (1-\eta)f^1_{k,n}(\mathbf{x}^I) - f^2_{k,n}(\mathbf{x},\eta), \end{aligned} \tag{13}$$

where

$$f^1_{k,n}(\mathbf{x}^I) \triangleq \ln\left(1+\frac{|\mathbf{h}^H_{k,k,n}\mathbf{x}^I_{k,n}|^2 - \epsilon_{k,k,n}\|\mathbf{x}^I_{k,n}\|^2}{\varphi_{k,n}(\mathbf{x}^I)}\right)$$

and

$$f^2_{k,n}(\mathbf{x},\eta) \triangleq \ln\left(1+\frac{\|\boldsymbol{\mathcal{H}}^H_{k,k}\mathbf{x}^I_{k,n}\|^2 + \epsilon_{k,k}\|\mathbf{x}^I_{k,n}\|^2}{q_{k,n}(\mathbf{x},\eta)}\right).$$

The corresponding rate can be expressed in units of bits/sec/Hz by evaluating $\frac{f_{k,n}(\mathbf{x},\eta)}{\ln 2}$.

At first, we aim to jointly optimize the transmit information and energy beamforming vectors, $\mathbf{x}^E_{k,n_1}$ and $\mathbf{x}^I_{k,n}$, respectively, and the TS ratio η to maximize the minimum secrecy rate

$$\max_{\substack{\mathbf{x}^E_{k,n_1},\mathbf{x}^I_{k,n}\in\mathbb{C}^{M\times 1}\\ \eta\in(0,1)}} F(\mathbf{x},\eta) \triangleq \min_{k\in\mathcal{K},n\in\mathcal{N}_k} f_{k,n}(\mathbf{x},\eta)$$

$$= \min_{k\in\mathcal{K},n\in\mathcal{N}_k} \Big[(1-\eta)f^1_{k,n}(\mathbf{x}^I) - f^2_{k,n}(\mathbf{x},\eta)\Big] \tag{14a}$$

$$\text{s.t. } g_k(\mathbf{x}_k) \triangleq \eta \sum_{n_1\in\mathcal{N}_{1,k}} \|\mathbf{x}^E_{k,n_1}\|^2 + (1-\eta)\sum_{n\in\mathcal{N}_k} \|\mathbf{x}^I_{k,n}\|^2 \le P^{\max}_k, \quad \forall k\in\mathcal{K}, \tag{14b}$$

$$g(\mathbf{x}) \triangleq \eta \sum_{k\in\mathcal{K}}\sum_{n_1\in\mathcal{N}_{1,k}} \|\mathbf{x}^E_{k,n_1}\|^2 + (1-\eta)\sum_{k\in\mathcal{K}}\sum_{n\in\mathcal{N}_k} \|\mathbf{x}^I_{k,n}\|^2 \le P^{\max}, \tag{14c}$$

$$p_{k,n_1}(\mathbf{x}^E) - \frac{e^{\min}_{k,n_1}}{\zeta_{k,n_1}\eta} \ge 0, \quad \forall k\in\mathcal{K},\ n_1\in\mathcal{N}_{1,k}, \tag{14d}$$

$$\|\mathbf{x}^E_{k,n_1}\|^2 \le P^{\max}_k, \quad \|\mathbf{x}^I_{k,n}\|^2 \le P^{\max}_k, \quad \forall k\in\mathcal{K}, \quad n\in\mathcal{N}_k, \tag{14e}$$

where $\mathbf{x}_k \triangleq [\mathbf{x}^E_{k,n_1}; \mathbf{x}^I_{k,n}]_{n_1\in\mathcal{N}_{1,k},n\in\mathcal{N}_k,\in\mathcal{K}}$.

Constraint (14b) is the individual cell transmit power budget, $P^{\max}_k$, at each BS k, while constraint (14c) is the total transmit power budget, $P^{\max}$, of the network. Constraint (14d) requires that the energy harvested by UE (k,n_1) is greater than some preset target threshold $e^{\min}_{k,n_1}$. Constraint (14e) is imposed to budget the beamforming power separately for each UE (k,n) during both EH and ID time periods. Note that the objective (14a) is non-concave while constraints (14b)-(14d) are non-convex due to coupling between the beamforming vectors $\mathbf{x}$ and time splitting factor η.

III. Proposed Path-following Computation

In order to solve the problem (14), we make the following change of variables:

$$1-\eta = \frac{1}{\mu}, \tag{15}$$

which implies the following linear constraint:

$$\mu > 1. \tag{16}$$

In what follows, we first transform the original max-min secrecy rate problem (14) by using the new variable μ.

A. Transformation of Problem (14) *by Using the Variable* μ

Using (15), the power constraints (14b) and (14c) become the following constraints:

$$\begin{aligned}\bar{g}_k(\mathbf{x}_k,\mu) \triangleq & \sum_{n_1\in\mathcal{N}_{1,k}} \|\mathbf{x}^E_{k,n_1}\|^2 + \frac{1}{\mu}\sum_{n\in\mathcal{N}_k}\|\mathbf{x}^I_{k,n}\|^2 \\ & -\frac{1}{\mu}\sum_{n_1\in\mathcal{N}_{1,k}}\|\mathbf{x}^E_{k,n_1}\|^2 \\ & \le P_k^{\max},\ \forall k\in\mathcal{K} \end{aligned} \tag{17a}$$

$$\begin{aligned}\bar{g}(\mathbf{x},\mu) \triangleq & \sum_{k\in\mathcal{K}}\sum_{n_1\in\mathcal{N}_{1,k}} \|\mathbf{x}^E_{k,n_1}\|^2 + \frac{1}{\mu}\sum_{k\in\mathcal{K}}\sum_{n\in\mathcal{N}_k}\|\mathbf{x}^I_{k,n}\|^2 \\ & -\frac{1}{\mu}\sum_{k\in\mathcal{K}}\sum_{n_1\in\mathcal{N}_{1,k}}\|\mathbf{x}^E_{k,n_1}\|^2 \\ & \le P^{\max}, \end{aligned} \tag{17b}$$

and applying (15) in (14d), the EH constraint (14d) in terms of μ will become

$$p_{k,n_1}(\mathbf{x}^E) \ge \frac{e^{\min}_{k,n_1}}{\zeta_{k,n_1}}\left(1+\frac{1}{\mu-1}\right)-\sigma_a^2. \tag{18}$$

Under the variable change (13), the achievable secrecy rate in terms of μ is given by

$$\bar{f}_{k,n}(\mathbf{x},\mu) = \frac{1}{\mu}f^1_{k,n}(\mathbf{x}^I) - \bar{f}^2_{k,n}(\mathbf{x},\mu) \tag{19}$$

where

$$\bar{f}^2_{k,n}(\mathbf{x},\mu) \triangleq \ln\left(1+\frac{\|\boldsymbol{\mathcal{H}}^H_{k,k}\mathbf{x}^I_{k,n}\|^2+\epsilon_{k,k}\|\mathbf{x}^I_{k,n}\|^2}{\bar{q}_{k,n}(\mathbf{x},\mu)}\right) \tag{20}$$

and by using $q_{k,n}(\mathbf{x},\eta)$ in (12), $\bar{q}_{k,n}(\mathbf{x},\mu)$ is defined as follows:

$$\begin{aligned}&\bar{q}_{k,n}(\mathbf{x},\mu) \\ &\triangleq (\mu-1)\left(\sum_{\bar{k}\in\mathcal{K}}\sum_{\bar{n}\in\mathcal{N}_{1,k}}\|\boldsymbol{\mathcal{H}}^H_{\bar{k},k}\mathbf{x}^E_{\bar{k},\bar{n}}\|^2 \right.\\ &\quad\left. -\sum_{\bar{k}\in\mathcal{K}}\sum_{\bar{n}\in\mathcal{N}_{1,k}}\epsilon_{\bar{k},k}\|\mathbf{x}^E_{\bar{k},\bar{n}}\|^2\right) \\ &\quad+\sum_{\bar{n}\in\mathcal{N}_k\setminus\{n\}}\|\boldsymbol{\mathcal{H}}^H_{k,k}\mathbf{x}^I_{k,\bar{n}}\|^2+\sum_{\bar{k}\in\mathcal{K}\setminus\{k\}}\sum_{\bar{n}\in\mathcal{N}_{\bar{k}}}\|\boldsymbol{\mathcal{H}}^H_{\bar{k},k}\mathbf{x}^I_{\bar{k},\bar{n}}\|^2 \\ &\quad-\left(\sum_{\bar{n}\in\mathcal{N}_k\setminus\{n\}}\epsilon_{k,k}\|\mathbf{x}^I_{k,\bar{n}}\|^2 \right.\\ &\quad\left.+\sum_{\bar{k}\in\mathcal{K}\setminus\{k\}}\sum_{\bar{n}\in\mathcal{N}_{\bar{k}}}\epsilon_{\bar{k},k}\|\mathbf{x}^I_{k,\bar{n}}\|^2\right)+\mu N_{\mathrm{ev}}\sigma_a^2. \end{aligned} \tag{21}$$

Using (17), (18), and (26), the equivalent to problem (14) in terms of $\mathbf{x}$ and μ is given by

$$\max_{\substack{\mathbf{x}^E_{k,n_1},\mathbf{x}^I_{k,n}\in\mathbb{C}^{M\times 1},\\ \mu}} \ \min_{\substack{k\in\mathcal{K},\\ n\in\mathcal{N}_k}}\left[\frac{1}{\mu}f^1_{k,n}(\mathbf{x}^I)-\bar{f}^2_{k,n}(\mathbf{x},\mu)\right] \tag{22a}$$

$$\text{s.t. (14e), (16), (17), (18).} \tag{22b}$$

B. Inner Approximation of Power Constraint (17) *and EH Constraint* (18)[4]

Let $(\mathbf{x}^{(\ell)},\mu^{(\ell)})$ be a feasible point for (22). By exploiting the convexity of $\frac{1}{\mu}\|\mathbf{x}\|^2$, the following inequality holds:

$$\begin{aligned}\frac{\|\mathbf{x}\|^2}{\mu} \ge & \frac{2\Re\left\{(\mathbf{x}^{(\ell)})^H\mathbf{x}\right\}}{\mu^{(\ell)}}-\frac{\|\mathbf{x}^{(\ell)}\|^2}{(\mu^{(\ell)})^2}\mu, \\ & \forall\mathbf{x}\in\mathbb{C}^N,\quad \mathbf{x}^{(\ell)}\in\mathbb{C}^N,\ \mu>0,\ \mu^{(\ell)}>0. \end{aligned} \tag{23}$$

Thus, using (23), inner convex approximations of the non-convex constraints (17a) and (17b) are given by

$$\begin{aligned}\bar{g}^{(\ell)}_k(\mathbf{x}_k,\mu) \triangleq & \sum_{n_1\in\mathcal{N}_{1,k}}\|\mathbf{x}^E_{k,n_1}\|^2+\frac{1}{\mu}\sum_{n\in\mathcal{N}_k}\|\mathbf{x}^I_{k,n}\|^2 \\ & -\frac{1}{\mu^{(\ell)}}\sum_{n_1\in\mathcal{N}_{1,k}}2\Re\left\{(\mathbf{x}^{E,(\ell)}_{k,n_1})^H\mathbf{x}^E_{k,n_1}\right\} \\ & +\frac{\mu}{(\mu^{(\ell)})^2}\sum_{n_1\in\mathcal{N}_{1,k}}\|\mathbf{x}^{E,(\ell)}_{k,n_1}\|^2 \\ & \le P_k^{\max},\quad \forall k\in\mathcal{K}, \end{aligned} \tag{24a}$$

$$\begin{aligned}\bar{g}^{(\ell)}(\mathbf{x},\mu) \triangleq & \sum_{k\in\mathcal{K}}\sum_{n_1\in\mathcal{N}_{1,k}}\|\mathbf{x}^E_{k,n_1}\|^2 \\ & +\frac{1}{\mu}\sum_{k\in\mathcal{K}}\sum_{n\in\mathcal{N}_k}\|\mathbf{x}^I_{k,n}\|^2 \\ & -\frac{1}{\mu^{(\ell)}}\sum_{k\in\mathcal{K}}\sum_{n_1\in\mathcal{N}_{1,k}}2\Re\left\{(\mathbf{x}^{E,(\ell)}_{k,n_1})^H\mathbf{x}^E_{k,n_1}\right\} \\ & +\frac{\mu}{(\mu^{(\ell)})^2}\sum_{k\in\mathcal{K}}\sum_{n_1\in\mathcal{N}_{1,k}}\|\mathbf{x}^{E,(\ell)}_{k,n_1}\|^2 \\ & \le P^{\max}. \end{aligned} \tag{24b}$$

Next, following the definition of $p_{k,n_1}(\mathbf{x}^E)$ in (3), and using the approximation

$$\begin{aligned}|\mathbf{h}^H_{\bar{k},k,n}\mathbf{x}_{\bar{k},\bar{n}}|^2 \ge & -|\mathbf{h}^H_{\bar{k},k,n}\mathbf{x}^{(\ell)}_{\bar{k},\bar{n}}|^2 \\ & +2\Re\left\{\left(\mathbf{x}^{(\ell)}_{\bar{k},\bar{n}}\right)^H\mathbf{h}_{\bar{k},k,n}\mathbf{h}^H_{\bar{k},k,n}\mathbf{x}_{\bar{k},\bar{n}}\right\} \\ & \forall\mathbf{x}_{\bar{k},\bar{n}},\mathbf{x}^{(\ell)}_{\bar{k},\bar{n}} \end{aligned} \tag{25}$$

an inner approximation of the constraint (18) is given by

$$\begin{aligned}&\sum_{\bar{k}\in\mathcal{K}}\sum_{\bar{n}\in\mathcal{N}_{1,\bar{k}}}\left[2\Re\left\{\mathbf{h}^H_{\bar{k},k,n_1}\mathbf{x}^{E,(\ell)}_{\bar{k},\bar{n}}\mathbf{h}^H_{\bar{k},k,n_1}\mathbf{x}^E_{\bar{k},\bar{n}}\right\}-\left|\mathbf{h}^H_{\bar{k},k,n_1}\mathbf{x}^{E,(\ell)}_{\bar{k},\bar{n}}\right|^2\right] \\ &\qquad\ge\frac{e^{\min}_{k,n_1}}{\zeta_{k,n_1}}\left(1+\frac{1}{\mu-1}\right)-\sigma_a^2. \end{aligned} \tag{26}$$

Using the convex approximations (24) and (26) for the constraints of problem (22), we obtain the following inner approximation at the ℓth iteration:

$$\max_{\substack{\mathbf{x}^E_{k,n_1},\mathbf{x}^I_{k,n}\in\mathbb{C}^{M\times 1},\\ \mu}} \ \min_{\substack{k\in\mathcal{K},\\ n\in\mathcal{N}_k}}\left[\frac{1}{\mu}f^1_{k,n}(\mathbf{x}^I)-\bar{f}^2_{k,n}(\mathbf{x},\mu)\right] \tag{27a}$$

$$\text{s.t. (14e), (16), (24a), (24b), (26).} \tag{27b}$$

[3]A constraint is called an inner approximation of another constraint if and only if any feasible point of the former is also feasible for the latter [47]

As observed in [48], for $\bar{\mathbf{x}}_{k,n}^I = e^{-\jmath.\arg(\mathbf{h}_{k,k,n}^H \mathbf{x}_{k,n}^I)}\mathbf{x}_{k,n}^I$, one has $|\mathbf{h}_{k,k,n}^H \mathbf{x}_{k,n}^I| = \mathbf{h}_{k,k,n}^H \bar{\mathbf{x}}_{k,n}^I = \Re\{\mathbf{h}_{k,k,n}^H \bar{\mathbf{x}}_{k,n}^I\} \geq 0$ and $|\mathbf{h}_{k',k,n'}^H \mathbf{x}_{k,n}^I| = |\mathbf{h}_{k',k,n'}^H \bar{\mathbf{x}}_{k,n}^I|$ for $(k', n') \neq (k, n)$ and $\jmath \triangleq \sqrt{-1}$. The problem (27) is thus equivalent to the following optimization problem:

$$\max_{\substack{\mathbf{x}_{k,n_1}^E, \mathbf{x}_{k,n}^I \in \mathbb{C}^{M\times 1}, \\ \mu}} \bar{F}(\mathbf{x}, \mu) \triangleq \min_{\substack{k\in\mathcal{K}, \\ n\in\mathcal{N}_k}} \bar{f}_{k,n}(\mathbf{x}, \mu)$$

$$= \min_{k\in\mathcal{K}, n\in\mathcal{N}_k} \left[\bar{f}_{k,n}^1(\mathbf{x}^I, \mu) - \bar{f}_{k,n}^2(\mathbf{x}, \mu)\right] \quad (28a)$$

$$\text{s.t. } \Re\left\{\mathbf{h}_{k,k,n}^H \mathbf{x}_{k,n}^I\right\} \geq 0, \quad \forall k \in \mathcal{K},\ n \in \mathcal{N}_k, \quad (28b)$$

$$(14e), (24a), (24b), (26), (16), \quad (28c)$$

where

$$\bar{f}_{k,n}^1(\mathbf{x}^I, \mu) \triangleq \frac{1}{\mu} \ln\left(1 + \frac{(\Re\{\mathbf{h}_{k,k,n}^H \mathbf{x}_{k,n}^I\})^2 - \epsilon_{k,k,n}\|\mathbf{x}_{k,n}^I\|^2}{\varphi_{k,n}(\mathbf{x}^I)}\right), \quad (29)$$

C. Lower Approximation of the Objective (28a)

For concave lower approximation of $\bar{f}_{k,n}(\mathbf{x}, \mu)$, which agrees with $\bar{f}_{k,n}$ at $\left(w^{(\ell)}, \mu^{(\ell)}\right)$, we provide a lower bounding concave function for the first term $\bar{f}_{k,n}^1(\mathbf{x}^I, \mu)$ and an upper bounding convex function for the second term $\bar{f}_{k,n}^2(\mathbf{x}, \mu)$. Recalling the definition (8) of $\varphi_{k,n}(\mathbf{x}^I)$, we have the following result.

Theorem 1: A lower bounding concave function $\bar{f}_{k,n}^{1,(\ell)}(\mathbf{x}^I, \mu)$ of $\bar{f}_{k,n}^1(\mathbf{x}^I, \mu)$, which agrees with $\bar{f}_{k,n}^1$ at $(\mathbf{x}_{k,n}^{I,(\ell)}, \mu^{(\ell)})$, is given by

$$\bar{f}_{k,n}^1(\mathbf{x}^I, \mu) \geq \bar{f}_{k,n}^{1,(\ell)}(\mathbf{x}^I, \mu) \triangleq a^{(\ell)} - b^{(\ell)} \frac{\varphi_{k,n}(\mathbf{x}^I)}{v_{k,n}(\mathbf{x}_{k,n}^I)} - c^{(\ell)}\mu \quad (30)$$

for

$$v_{k,n}(\mathbf{x}_{k,n}^I) \leq \psi_{k,n}(\mathbf{x}_{k,n}^I) - \epsilon_{k,k,n}\|\mathbf{x}_{k,n}^I\|^2, \quad \forall k \in \mathcal{K},\ n \in \mathcal{N}_k, \quad (31a)$$

$$v_{k,n} \geq 0, \quad \psi_{k,n} \geq 0, \ \forall k \in \mathcal{K},\ n \in \mathcal{N}_k, \quad (31b)$$

where

$$a^{(\ell)} = 2\frac{\ln(1+d^{(\ell)})}{\mu^{(\ell)}} + \frac{d^{(\ell)}}{\mu^{(\ell)}(d^{(\ell)}+1)} > 0,$$

$$b^{(\ell)} = \frac{(d^{(\ell)})^2}{\mu^{(\ell)}(d^{(\ell)}+1)} > 0,$$

$$c^{(\ell)} = \frac{\ln(1+d^{(\ell)})}{(\mu^{(\ell)})^2} > 0,$$

$$d^{(\ell)} = ((\Re\{\mathbf{h}_{k,k,n}^H \mathbf{x}_{k,n}^{I,(\ell)}\})^2 - \epsilon_0||\mathbf{x}_{k,n}^{I,(\ell)}||^2)/\varphi_{k,n}(\mathbf{x}^{I,(\ell)}) \quad (32)$$

and

$$\psi_{k,n}(\mathbf{x}_{k,n}^I) \triangleq 2\Re\{\mathbf{h}_{k,k,n}^H \mathbf{x}_{k,n}^{I,(\ell)}\}\Re\left\{\mathbf{h}_{k,k,n}^H \mathbf{x}_{k,n}^I\right\} - \left(\Re\left\{\mathbf{h}_{k,k,n}^H \mathbf{x}_{k,n}^{I,(\ell)}\right\}\right)^2. \quad (33)$$

The upper bounding convex function $\bar{f}_{k,n}^{2,(\ell)}(\mathbf{x}, \mu)$ on $\bar{f}_{k,n}^2(\mathbf{x}, \mu)$, which agrees with $\bar{f}_{k,n}^2$ at $(\mathbf{x}^{(\ell)}, \mu^{(\ell)})$, is given by

$$\begin{aligned}\bar{f}_{k,n}^2(\mathbf{x}, \mu) &\leq \bar{f}_{k,n}^{2,(\ell)}(\mathbf{x}, \mu) \\ &\triangleq \bar{f}_{k,n}^2(w^{(\ell)}, \mu^{(\ell)}) \\ &\quad + \left(1 + \frac{\|\boldsymbol{\mathcal{H}}_{k,k}^H w_{k,n}^{I,(\ell)}\|^2 + \epsilon_{k,k}\|w_{k,n}^{I,(\ell)}\|^2}{\bar{q}_{k,n}(w^{(\ell)}, \mu^{(\ell)})}\right)^{-1} \\ &\quad \times \left(\frac{\|\boldsymbol{\mathcal{H}}_{k,k}^H \mathbf{x}_{k,n}^I\|^2 + \epsilon_{k,k}\|\mathbf{x}_{k,n}^I\|^2}{\sqrt{\beta_{k,n}}}\right. \\ &\quad \left. - \frac{\|\boldsymbol{\mathcal{H}}_{k,k}^H w_{k,n}^{I,(\ell)}\|^2 + \epsilon_{k,k}\|w_{k,n}^{I,(\ell)}\|^2}{\bar{q}_{k,n}(w^{(\ell)}, \mu^{(\ell)})}\right) \end{aligned} \quad (34)$$

where

$$\beta_{k,n} > 0, \quad q\forall\ k \in \mathcal{K},\ n \in \mathcal{N}_k \quad (35)$$

$$\sqrt{\beta_{k,n}} \leq \bar{q}_{k,n}(\mathbf{x}, \mu), \quad \forall\ k \in \mathcal{K},\ n \in \mathcal{N}_k, \quad (36)$$

where constraint (36) is innerly approximated by the constraint

$$\frac{1}{2}\left(\frac{\beta_{k,n}}{\sqrt{\beta_{k,n}^{(\ell)}}(\mu^{(\ell)}-1)} + \frac{\sqrt{\beta_{k,n}^{(\ell)}}(\mu^{(\ell)}-1)}{(\mu-1)^2}\right) \leq \bar{q}_{k,n}^{(\ell)}(\mathbf{x}, \mu) \quad (37)$$

and

$$2\mu^{(\ell)} - 1 - \mu > 0. \quad (38)$$

for

$$\sqrt{\beta_{k,n}^{(\ell)}} = \bar{q}_{k,n}(\mathbf{x}^{(\ell)}, \mu^{(\ell)}) \quad (39)$$

and

$$\begin{aligned}\bar{q}_{k,n}^{(\ell)}(\mathbf{x}, \mu) \triangleq &-\frac{1}{\mu-1}\left(\sum_{\bar{n}\in\mathcal{N}_k\setminus\{n\}} \epsilon_{k,k}\|\mathbf{x}_{k,\bar{n}}^I\|^2\right. \\ &\left. + \sum_{\bar{k}\in\mathcal{K}\setminus\{k\}}\sum_{\bar{n}\in\mathcal{N}_{\bar{k}}} \epsilon_{\bar{k},k}\|\mathbf{x}_{\bar{k},\bar{n}}^I\|^2\right) - \sum_{\bar{k}\in\mathcal{K}}\sum_{\bar{n}\in\mathcal{N}_{1,k}} \epsilon_{\bar{k},k}\|\mathbf{x}_{\bar{k},\bar{n}}^E\|^2 \\ &+ \sum_{\bar{k}\in\mathcal{K}}\sum_{\bar{n}\in\mathcal{N}_{1,k}} \Re\left\{\left\langle \boldsymbol{\mathcal{H}}_{\bar{k},k}^H \mathbf{x}_{\bar{k},\bar{n}}^{E,(\ell)}, 2\boldsymbol{\mathcal{H}}_{\bar{k},k}^H \mathbf{x}_{\bar{k},\bar{n}}^{E,(\ell)} \mathbf{x}_{\bar{k},\bar{n}}^E \right.\right. \\ &\left.\left. - \boldsymbol{\mathcal{H}}_{\bar{k},k}^H \mathbf{x}_{\bar{k},\bar{n}}^{E,(\ell)} \right\rangle\right\} \\ &+ \frac{2}{\mu^{(\ell)}-1}\left(\sum_{\bar{n}\in\mathcal{N}_k\setminus\{n\}} \Re\left\{\left\langle \boldsymbol{\mathcal{H}}_{k,k}^H \mathbf{x}_{k,\bar{n}}^{I,(\ell)}, \boldsymbol{\mathcal{H}}_{k,k}^H \mathbf{x}_{k,\bar{n}}^I \right\rangle\right\}\right. \\ &\left. + \sum_{\bar{k}\in\mathcal{K}\setminus\{k\}}\sum_{\bar{n}\in\mathcal{N}_{\bar{k}}} \Re\left\{\left\langle \boldsymbol{\mathcal{H}}_{\bar{k},k}^H \mathbf{x}_{\bar{k},\bar{n}}^{I,(\ell)}, \boldsymbol{\mathcal{H}}_{\bar{k},k}^H \mathbf{x}_{\bar{k},\bar{n}}^I \right\rangle\right\}\right) \\ &- \frac{\mu-1}{(\mu^{(\ell)}-1)^2}\left(\sum_{\bar{n}\in\mathcal{N}_k\setminus\{n\}} \|\boldsymbol{\mathcal{H}}_{k,k}^H \mathbf{x}_{k,\bar{n}}^{I,(\ell)}\|^2\right. \\ &\left. + \sum_{\bar{k}\in\mathcal{K}\setminus\{k\}}\sum_{\bar{n}\in\mathcal{N}_{\bar{k}}} \|\boldsymbol{\mathcal{H}}_{\bar{k},k}^H \mathbf{x}_{\bar{k},\bar{n}}^{I,(\ell)}\|^2\right) \\ &+ \left(1 + \frac{2}{\mu^{(\ell)}-1} - \frac{\mu-1}{(\mu^{(\ell)}-1)^2}\right) N_{\text{ev}}\sigma_a^2. \end{aligned} \quad (40)$$

Proof: See the appendix. ■

Thus, by applying Theorem 1, we can use the following convex quadratic program (QP) to achieve minorant maximization for the non-convex problem (28) at a feasible $(\mathbf{x}_{k,n}^{E,(\ell)}, \mathbf{x}_{k,n}^{I,(\ell)}, \mu^{(\ell)})$:

$$\max_{\substack{\mathbf{x}_{k,n_1}^E, \mathbf{x}_{k,n}^I \in \mathbb{C}^{M\times 1},\\ \mu}} \min_{\substack{k\in\mathcal{K},\\ n\in\mathcal{N}_k}} \left[\bar{f}_{k,n}^{1,(\ell)}(\mathbf{x}^I, \mu) - \bar{f}_{k,n}^{2,(\ell)}(\mathbf{x}, \mu)\right] \quad (41a)$$

$$\text{s.t. (14e), (24a), (24b), (26), (16), (28b),}$$
$$(31), (35), (37), (38). \quad (41b)$$

Algorithm 1 Path-Following Algorithm for Secrecy Rate Optimization (14)

1: Initialize $\ell := 0$.
2: Find a feasible point $\left(\mathbf{x}^{E,(0)}, \mathbf{x}^{I,(0)}, \mu^{(0)}\right)$ of (22).
3: **repeat**
4: Solve the convex problem (41) to find $\left(\mathbf{x}^{E,(\ell+1)}, \mathbf{x}^{I,(\ell+1)}, \mu^{(\ell+1)}\right)$.
5: Set $\ell := \ell + 1$.
6: **until** the objective in (22) converges.

D. Details of Proposed Algorithm 1 With Its Initialization

The proposed computation for the max-min secrecy rate problem (22) (and hence (14)) is summarized in Algorithm 1. Since the objective function in (41) agrees with that in (22) at $(\mathbf{x}^{(\ell)}, \mu^{(\ell)})$, which is also feasible for (41), it follows that

$$\begin{aligned}
&\min_{\substack{k\in\mathcal{K},\\ n\in\mathcal{N}_k}} \left[\frac{1}{\mu^{(\ell+1)}}\bar{f}_{k,n}^1(\mathbf{x}^{I,(\ell+1)}) - \bar{f}_{k,n}^2(\mathbf{x}^{(\ell+1)}, \mu^{(\ell+1)})\right] \\
&\geq \min_{\substack{k\in\mathcal{K},\\ n\in\mathcal{N}_k}} \left[\bar{f}_{k,n}^{1,(\ell)}(\mathbf{x}^{I,(\ell+1)}, \mu^{(\ell+1)}) - \bar{f}_{k,n}^{2,(\ell)}(\mathbf{x}^{(\ell+1)}, \mu^{(\ell+1)})\right] \\
&> \min_{\substack{k\in\mathcal{K},\\ n\in\mathcal{N}_k}} \left[\bar{f}_{k,n}^{1,(\ell)}(\mathbf{x}^{I,(\ell)}, \mu^{(\ell)}) - \bar{f}_{k,n}^{2,(\ell)}(\mathbf{x}^{(\ell)}, \mu^{(\ell)})\right] \\
&= \min_{\substack{k\in\mathcal{K},\\ n\in\mathcal{N}_k}} \left[\frac{1}{\mu^{(\ell)}}\bar{f}_{k,n}^1(\mathbf{x}^{I,(\ell)}) - \bar{f}_{k,n}^2(\mathbf{x}^{(\ell)}, \mu^{(\ell)})\right], \quad (42)
\end{aligned}$$

i.e. $(\mathbf{x}^{(\ell+1)}, \mu^{(\ell+1)})$ is a feasible point, which is better than $(\mathbf{x}^{(\ell)}, \mu^{(\ell)})$ for (22), whenever $(\mathbf{x}^{(\ell+1)}, \mu^{(\ell+1)}) \neq (\mathbf{x}^{(\ell)}, \mu^{(\ell)})$. On the other hand, if $(\mathbf{x}^{(\ell+1)}, \mu^{(\ell+1)}) = (\mathbf{x}^{(\ell)}, \mu^{(\ell)})$, i.e. $(\mathbf{x}^{(\ell)}, \mu^{(\ell)})$ is the optimal solution of the convex optimization problem (41) then it must satisfy the first order necessary optimality condition for (41), which obviously is also the first order necessary optimality condition for (22). We have thus proved that the sequence $\{(\mathbf{x}^{(\ell)}, \mu^{(\ell)})\}$ converges to a point satisfying the first order necessary optimality condition for the non-convex optimization problem (22).

A feasible point $\left(\mathbf{x}^{E,(0)}, \mathbf{x}^{I,(0)}, \mu^{(0)}\right)$ for (22) (and hence (14)) for initializing Algorithm 1 is found as as follows. We first fix $\mu^{(0)}$ and solve the following convex problem:

$$\max_{\substack{\mathbf{x}_{k,n}^x \in \mathbb{C}^{M\times 1},\\ x\in\{I,E\}}} \min_{\substack{k\in\mathcal{K},\\ n\in\mathcal{N}_k}} \Re\left\{\mathbf{h}_{k,k,n}^H \mathbf{x}_{k,n_1}^E\right\} - \sqrt{e_{k,n}^{\min}/\left(\zeta_{k,n}\left(1 - 1/\mu^{(0)}\right)\right)} \quad (43a)$$

$$\text{s.t. } \|\mathbf{x}_{k,n_1}^E\|^2 \leq P_k^{\max}, \quad \|\mathbf{x}_{k,n}^I\|^2 \leq P_k^{\max}, \quad (43b)$$

$$\forall k \in \mathcal{K}, \quad n \in \mathcal{N}_k,$$

$$\Re\left\{\mathbf{h}_{k,k,n}^H \mathbf{x}_{k,n}^I\right\} \geq \sqrt{e^{r^{\min}\mu^{(0)}} - 1} \times \left\| \left(\mathbf{h}_{\bar{k},k,n}^H \mathbf{x}_{\bar{k},\bar{n}}^I\right)_{\bar{k},\bar{n}\in\mathcal{K},\mathcal{N}\setminus\{k,n\}} \right\|_2, \quad (43c)$$

$$k \in \mathcal{K}, n \in \mathcal{N},$$

$$\bar{g}_k\left(\mathbf{x}_k, \mu^{(0)}\right) \leq P_k^{\max}, \quad \forall k \in \mathcal{K}, \quad (43d)$$

$$\bar{g}\left(\mathbf{x}, \mu^{(0)}\right) \leq P^{\max}, \quad (43e)$$

where, for rapid convergence, the constraint (43c) on the information rate of UE (k, n) is imposed. Note that the constraint (18) is satisfied if the objective function (43a) is positive. The constraint (43c) is a second-order cone constraint [49]. Using the optimal solution $\mathbf{x}_{k,n}^{E,(0)}$ of (43) as the initial point, we then iteratively solve the following convex program:

$$\begin{aligned}
&\max_{\substack{\mathbf{x}_{k,n}^x \in \mathbb{C}^{M\times 1},\\ x\in\{I,E\}}} \min_{\substack{k\in\mathcal{K},\\ n\in\mathcal{N}_k}} \sum_{\bar{k}\in\mathcal{K}} \sum_{\bar{n}\in\mathcal{N}_{\bar{k}}} \left[2\Re\left\{\mathbf{h}_{\bar{k},k,n}^H \mathbf{x}_{\bar{k},\bar{n}}^{E,(\ell)} \mathbf{h}_{\bar{k},k,n}^H \mathbf{x}_{\bar{k},\bar{n}}^E\right\} - \left|\mathbf{h}_{\bar{k},k,n}^H \mathbf{x}_{\bar{k},\bar{n}}^{E,(\ell)}\right|^2\right] - \frac{e_{k,n}^{\min}}{\zeta_{k,n}}\left(1 + \frac{1}{\mu^{(0)} - 1}\right) - \sigma_a^2 \\
&\text{s.t. (43b), (43c), (43d), (43e).} \quad (44)
\end{aligned}$$

until a positive value of the objective function is achieved. If either problem (43) is found infeasible or a positive value is not found by solving (44), we use a different value of $\mu^{(0)}$ and repeat the above process until a feasible point $\left(\mathbf{x}^{E,(0)}, \mathbf{x}^{I,(0)}, \mu^{(0)}\right)$ is obtained.[4]

IV. Energy Efficient Secure Beamforming

This section extends the proposed robust secrecy rate maximization algorithm to solve the secrecy energy efficiency maximization problem, which is formulated in the presence of channel estimation errors and eavesdroppers as

$$\max_{\substack{\mathbf{x}_{k,n_1}^E, \mathbf{x}_{k,n}^I \in \mathbb{C}^{M\times 1}\\ \eta\in(0,1)}} \min_{k\in\mathcal{K}} \frac{\sum_{n\in\mathcal{N}_k}\left[(1-\eta) f_{k,n}^1(\mathbf{x}^I) - f_{k,n}^2(\mathbf{x}, \eta)\right]}{\frac{1}{\xi} g_k(\mathbf{x}_k, \eta) + MP_A + P_c}$$

$$\text{s.t. (14}b\text{), (14}c\text{), (14}d\text{), (14}e\text{),} \quad (45a)$$

$$(1-\eta) f_{k,n}^1(\mathbf{x}^I) - f_{k,n}^2(\mathbf{x}, \eta) \geq r_{k,n}, \quad \forall\, k \in \mathcal{K},\ n \in \mathcal{N}_k, \quad (45b)$$

where ξ is the constant power amplifier efficiency, P_A is the power dissipation at each transmit antenna, P_c is the fixed circuit power consumption for base-band processing and $r_{k,n}$ is the threshold secrecy rate to ensure quality of service. The security and energy efficiency are combined into a single objective in (45a) to express the SEE in terms of secrecy bits per Joule per Hertz.

[4]Our simulation results in Sec. V show that the initialization problems (43) and (44) are feasible, and in almost all of the scenarios considered, we achieve a positive optimal value of (44) in one single iteration and with the first tried value of $\mu^{(0)} = 1.11$.

The conventional approach to address (45) (see e.g. [31], [32]) is based on Dinkelbach's method of fractional programming [30] to find $\tau > 0$ such that the optimal value of the following optimization problem is zero:

$$\max_{\substack{\mathbf{x}^E_{k,n_1},\mathbf{x}^I_{k,n}\in\mathbb{C}^{M\times 1}\\ \eta\in(0,1)}} \min_{k\in\mathcal{K}} \left\{ \sum_{n\in\mathcal{N}_k} [(1-\eta) f^1_{k,n}(\mathbf{x}^I) - f^2_{k,n}(\mathbf{x},\eta)] - \tau[\frac{1}{\xi} g_k(\mathbf{x}_k,\eta) + MP_A + P_c] \right\}$$
$$\text{s.t. } (14b), (14c), (14d), (14e), (45b). \tag{46}$$

However, for each fixed $\tau > 0$, the optimization problem (46) is non-convex convex and thus is still difficult computationally. It is important to realize that the original Dinkelbach method [30] is attractive only for maximizing a ratio of a convex and concave functions over a convex set, under which each subproblem for fixed τ is an easy convex optimization problem. It is not useful whenever either the objective is not a ratio of concave and convex functions or the constraint set is not convex.

We now develop an efficient path-following computational procedure for solving (45), which bypasses the difficult optimization problem (46). Using the variable change (16) again, this problem is equivalent to

$$\max_{\substack{\mathbf{x}^E_{k,n_1},\mathbf{x}^I_{k,n}\in\mathbb{C}^{M\times 1}\\ \mu>1,t_k>0}} \min_{k\in\mathcal{K}} \sum_{n\in\mathcal{N}_k} [\frac{f^1_{k,n}(\mathbf{x}^I)}{\mu\sqrt{t_k}} - \frac{\bar{f}^2_{k,n}(\mathbf{x},\mu)}{\sqrt{t_k}}] \tag{47a}$$
$$\text{s.t. } (14e), (17), (18), (16),$$
$$\bar{f}^1_{k,n}(\mathbf{x}^I,\mu) - \bar{f}^2_{k,n}(\mathbf{x},\mu) \geq r_{k,n} \quad \forall k\in\mathcal{K},\ n\in\mathcal{N}_k, \tag{47b}$$
$$\frac{1}{\xi}\bar{g}_k(\mathbf{x}_k,\mu) + MP_A + P_c \leq \sqrt{t_k}, \quad \forall\, k\in\mathcal{K}. \tag{47c}$$

By using (30) we obtain

$$\begin{aligned}\frac{f^1_{k,n}(\mathbf{x}^I)}{\mu\sqrt{t_k}} &\geq A^{(\ell)} - B^{(\ell)}\frac{\varphi_{k,n}(\mathbf{x}^I)}{v_{k,n}(\mathbf{x}^I_{k,n})} - C^{(\ell)}\mu\sqrt{t_k}\\ &\geq \Phi^{(\ell)}_{k,n}(\mathbf{x},\mu,t_k)\\ &\triangleq A^{(\ell)} - B^{(\ell)}\frac{\varphi_{k,n}(\mathbf{x}^I)}{v_{k,n}(\mathbf{x}^I_{k,n})}\\ &\quad - C^{(\ell)}\left(\frac{\sqrt{t^{(\ell)}_k}}{2\mu^{(\ell)}}\mu^2 + \frac{\mu^{(\ell)}}{2\sqrt{t^{(\ell)}_k}}t_k\right)\end{aligned} \tag{48}$$

for (31), where $\sqrt{t^{(\ell)}_k} = \bar{g}_k(\mathbf{x}^{(\ell)}_k,\mu^{(\ell)}) + MP_A + P_c$ and

$$A^{(\ell)} = 2\frac{\ln(1+D^{(\ell)})}{\mu^{(\ell)}\sqrt{t^{(\ell)}_k}} + \frac{D^{(\ell)}}{\mu^{(\ell)}\sqrt{t^{(\ell)}_k}(D^{(\ell)}+1)} > 0,$$
$$B^{(\ell)} = \frac{(D^{(\ell)})^2}{\mu^{(\ell)}\sqrt{t^{(\ell)}_k}(D^{(\ell)}+1)} > 0,$$
$$C^{(\ell)} = \frac{\ln(1+D^{(\ell)})}{[\mu^{(\ell)}\sqrt{t^{(\ell)}_k}]^2} > 0,$$
$$D^{(\ell)} = ((\Re\{\mathbf{h}^H_{k,k,n}\mathbf{x}^{I,(\ell)}_{k,n}\})^2 - \epsilon_0||\mathbf{x}^{I,(\ell)}_{k,n}||^2)/\varphi_{k,n}(\mathbf{x}^{I,(\ell)}).$$

Similarly to (34), we have

$$\begin{aligned}\frac{\bar{f}^2_{k,n}(\mathbf{x},\mu)}{\sqrt{t_k}} &\leq \frac{\bar{f}^2_{k,n}(w^{(\ell)},\mu^{(\ell)})}{\sqrt{t_k}}\\ &\quad + \left(1 + \frac{\|\boldsymbol{\mathcal{H}}^H_{k,k}w^{I,(\ell)}_{k,n}\|^2 + \epsilon_{k,k}\|w^{I,(\ell)}_{k,n}\|^2}{\bar{q}_{k,n}(w^{(\ell)},\mu^{(\ell)})}\right)^{-1}\\ &\quad \times \left(\frac{\|\boldsymbol{\mathcal{H}}^H_{k,k}\mathbf{x}^I_{k,n}\|^2 + \epsilon_{k,k}\|\mathbf{x}^I_{k,n}\|^2}{\sqrt{t_k\beta_{k,n}}}\right.\\ &\quad \left. - \frac{\|\boldsymbol{\mathcal{H}}^H_{k,k}w^{I,(\ell)}_{k,n}\|^2 + \epsilon_{k,k}\|w^{I,(\ell)}_{k,n}\|^2}{\bar{q}_{k,n}(w^{(\ell)},\mu^{(\ell)})\sqrt{t_k}}\right)\end{aligned} \tag{49}$$
$$\leq \Psi^{(\ell)}_{k,n}(\mathbf{x},\mu,t_k), \tag{50}$$

with (35), (36) and

$$0 < t_k \leq 3t^{(\ell)}_k, \quad \forall\, k\in\mathcal{K}, \tag{51}$$

where

$$\begin{aligned}&\Psi^{(\ell)}_{k,n}(\mathbf{x},\mu,t_k)\\ &\triangleq \frac{\bar{f}^2_{k,n}(w^{(\ell)},\mu^{(\ell)})}{\sqrt{t_k}}\\ &\quad + \left(1 + \frac{\|\boldsymbol{\mathcal{H}}^H_{k,k}w^{I,(\ell)}_{k,n}\|^2 + \epsilon_{k,k}\|w^{I,(\ell)}_{k,n}\|^2}{\bar{q}_{k,n}(w^{(\ell)},\mu^{(\ell)})}\right)^{-1}\\ &\quad \times \left(\frac{\|\boldsymbol{\mathcal{H}}^H_{k,k}\mathbf{x}^I_{k,n}\|^2 + \epsilon_{k,k}\|\mathbf{x}^I_{k,n}\|^2}{\sqrt{t_k\beta_{k,n}}}\right.\\ &\quad \left. - \frac{\|\boldsymbol{\mathcal{H}}^H_{k,k}w^{I,(\ell)}_{k,n}\|^2 + \epsilon_{k,k}\|w^{I,(\ell)}_{k,n}\|^2}{2\bar{q}_{k,n}(w^{(\ell)},\mu^{(\ell)})\sqrt{t^{(\ell)}_k}}\left(3 - \frac{t_k}{t^{(\ell)}_k}\right)\right).\end{aligned} \tag{52}$$

For the approximation (50) under (51), we have used the following inequality:

$$\frac{1}{\sqrt{t}} \geq \frac{1}{2\sqrt{\bar{t}}}\left(3 - \frac{t}{\bar{t}}\right) \quad \forall\ t>0,\ \bar{t}>0.$$

The inner approximations in (48) and (50) can be easily followed by using the procedure in the appendix. The following convex program is minorant maximization for the non-convex program (47):

$$\max_{\substack{\mathbf{x}^E_{k,n_1},\mathbf{x}^I_{k,n}\in\mathbb{C}^{M\times 1}\\ \mu>1,t_k>0}} \min_{k\in\mathcal{K}} \sum_{n\in\mathcal{N}_k} [\Phi^{(\ell)}_{k,n}(\mathbf{x},\mu,t_k)) - \Psi^{(\ell)}_{k,n}(\mathbf{x},\mu,t_k)] \tag{53a}$$
$$\text{s.t. } (14e), (24a), (24b), (26), (16), (28b), (31),$$
$$(35), (51), (37), (38), \tag{53b}$$
$$\bar{f}^{1,(\ell)}_{k,n}(\mathbf{x}^I,\mu) - \bar{f}^{2,(\ell)}_{k,n}(\mathbf{x},\mu) \geq r_{k,n}, \quad \forall\, k\in\mathcal{K},\ n\in\mathcal{N}_k, \tag{53c}$$
$$\frac{1}{\xi}\bar{g}^{(\ell)}_k(\mathbf{x}_k,\mu) + MP_A + P_c \leq \sqrt{t_k}, \quad \forall\, k\in\mathcal{K}. \tag{53d}$$

Algorithm 2 outlines the steps to solve the max-min energy efficiency problem (47) (and hence (45)). Similar to Algorithm 1, Algorithm 2 generates a sequence $\{(\mathbf{x}^{E,(\ell)},\mathbf{x}^{I,(\ell)},\mathbf{t}^{(\ell)},\mu^{(\ell)})\}$ of improved points of (53), which converges to a Karush-Kuhn-Tucker point, where

Algorithm 2 Path-following Algorithm for SEE Optimization (45)

1: Initialize $\ell := 0$.
2: Find a feasible point $\left(\mathbf{x}^{E,(0)}, \mathbf{x}^{I,(0)}, \mathbf{t}^{(0)}, \mu^{(0)}\right)$ of (47).
3: **repeat**
4: Solve the convex program (53) for $\left(\mathbf{x}^{E,(\ell+1)}, \mathbf{x}^{I,(\ell+1)}, \mathbf{t}^{(\ell+1)}\mu^{(\ell+1)}\right)$.
5: Set $\ell := \ell + 1$.
6: **until** the objective in (47) converges.

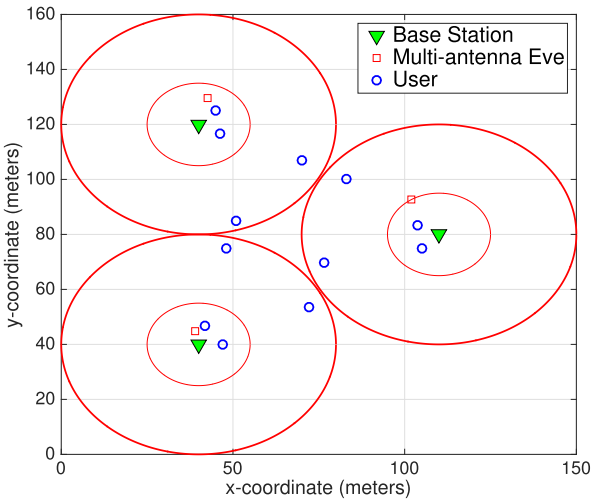

Fig. 2. The multicell network setting used in our numerical examples.

$\mathbf{t}^{(\ell)} \triangleq [t_1^{(\ell)}, \ldots, t_K^{(\ell)}]^T$. A feasible point $\left(\mathbf{x}^{E,(0)}, \mathbf{x}^{I,(0)}, \mathbf{t}^{(0)}, \mu^{(0)}\right)$ of (27) (and hence (45)) for initializing Algorithm 2 can be obtained by first solving (43) and (44) followed by the feasibility problem (53b), (53c), and (53d). It was already noted in Section III how efficiently the solution of (43) and (44) is obtained. The solution to the feasibility problem (53b), (53c), and (53d) is mostly obtained at the first iteration.

V. Simulation Results

To analyze the proposed algorithms through simulations, a network topology as shown in Fig. 2 is set up. There are $K = 3$ cells and $N = N_k = 4$, $\forall\ k \in \mathcal{K}$, UEs per cell with two placed inside the inner-circle in zone-1 and the remaining two placed in the outer zone near cell-edges, i.e., $N_{1,k} = N_{2,k} = 2$, $\forall\ k$. The cell radius is set to be 40m with an inner circle radius of 15m. A single $N_{\text{ev}} = 2$-antennas eavesdropper is randomly placed inside the inner circle in each cell. The path loss exponent is set to be $\mu = 3$. We generate Rician fading channels with Rician factor $K_R = 10$ dB [3]. For simplicity, we set $e_{k,n_1}^{\min} \equiv e^{\min}$ for the energy harvesting thresholds and $\zeta_{k,n_1} \equiv \zeta$, $\forall k, n_1$, for the energy harvesting conversion efficiency. Further, we set the energy conversion efficiency $\zeta = 0.5$, noise variance $\sigma_a^2 = -90$ dBm (unless specified otherwise), and maximum BS transmit power $P_k^{\max} = 26$ dBm, $\forall\ k$, which is in line with the frequently made assumption for the power budget of small-cell BSs [50]. We choose the value $P^{\max} = 30$ dBm as the power budget for the entire network. Unless stated otherwise, we choose the uncertainty in eavesdroppers' and neighboring users' channels as $\epsilon_0 = 0.005$, and we choose the uncertainty in serving users' channels as $\epsilon_1 = 10^{-3}$. It is reasonable to assume that BSs can achieve good channel estimates for their serving cell users compared to the neighboring cell users in a dense small cell network. Later in this section, we also investigate the effect of different values of channel uncertainties on the achievable secrecy rate. For the energy efficiency maximization problem in Section IV, we choose the power amplifier efficiency $\xi = 0.2$, the power dissipation at each transmit antenna $P_A = 0.6$W (27.78 dBm), and the circuit power consumption $P_c = 2.5$W (33.97 dBm) [37], [51]. We set the threshold secrecy rate $r_{k,n} = 0.1$ bits/sec/Hz for $M = 4$ BS antennas and otherwise $r_{k,n} = 0.5$ bits/sec/Hz for $M \in \{5, 6\}$ BS antennas.

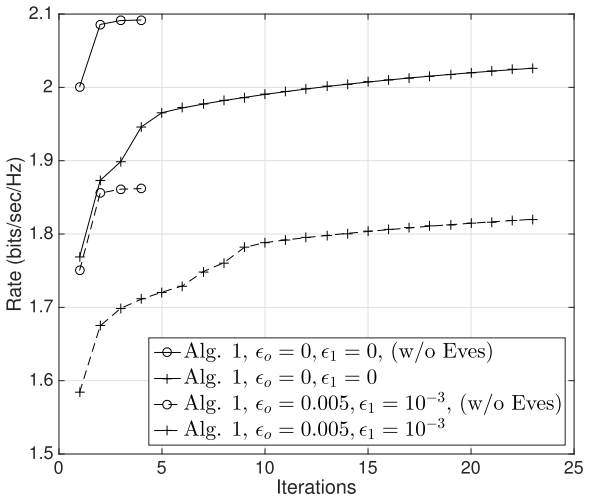

Fig. 3. Convergence of Algorithm 1 for $M = 5$ and $e^{\min} = -20$ dBm.

The convergence of Algorithm 1 for $M = 5$ BS antennas and minimum energy harvesting threshold $e^{\min} = -20$ dBm is shown by Fig. 3. We can see that whether we assume perfect channel estimation $\epsilon_0 = 0$, $\epsilon_1 = 0$ or assume some channel uncertainty $\epsilon_0 = 0.005$, $\epsilon_0 = 10^{-3}$, Algorithm 1 converges within $20 - 25$ iterations. We also observe that if we assume the absence of eavesdroppers, Algorithm 1 quickly converges in about four iterations. On average, Algorithm 1 requires 22.5 iterations before convergence, while the absence of eavesdroppers reduces the average required number of iterations to 3.5. The slower convergence in the presence of eavesdroppers is expected since then, not only does the objective (41a) become quite complicated, but also new constraints, (35), (37), and (38) must be satisfied.

The worst secrecy and normal rates (in the absence of eavesdroppers) for both perfect channel estimation $\epsilon_0 = 0$, $\epsilon_1 = 0$, and with the presence of channel uncertainty of $\epsilon_0 = 0.005, \epsilon_1 \in 10^{-3}$, are shown in Figs. 4 and 5. The normal rate excludes eavesdroppers and accordingly the optimization problem (14) with $f_{k,n}^2(\mathbf{x}, \eta) \equiv 0$ in (14a) is solved. The dashed curves in Figs. 4 and 5 correspond to the presence of channel uncertainties, while the solid curves correspond to the absence of channel uncertainty $\epsilon_0 = 0$, $\epsilon_1 = 0$. We can observe from Figs. 4 and 5 that the proposed robust secrecy rate algorithm performs quite well in the presence of channel

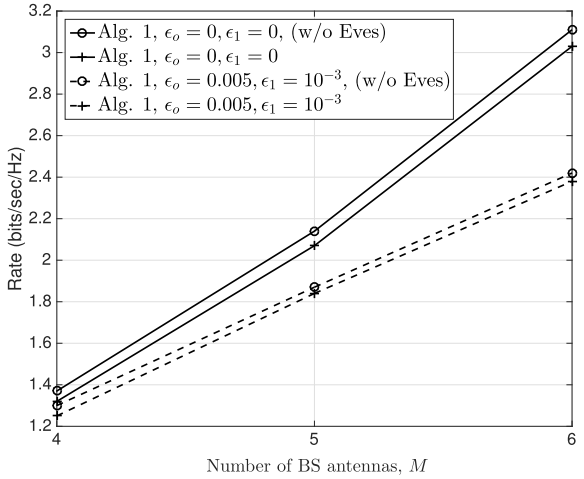

Fig. 4. Robust secrecy rate and normal rate in the presence and absence of eavesdroppers, respectively, for varying numbers of antennas M and different levels of channel uncertainties, but fixed EH threshold $e^{\min} = -20$ dBm.

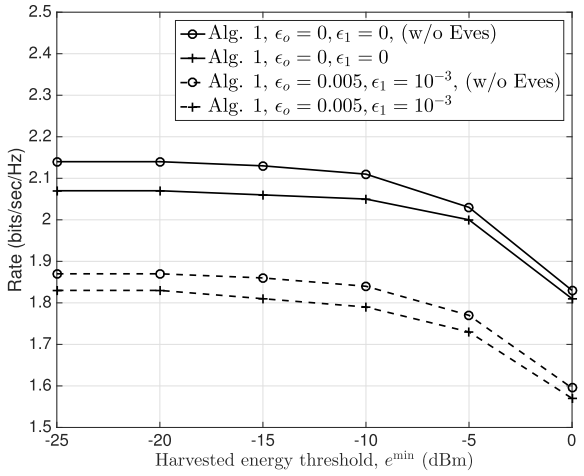

Fig. 5. Robust secrecy rate and normal rate in the presence and absence of eavesdroppers, respectively, for different values of EH thresholds $e^{\min}$ and different levels of channel uncertainties, but fixed number of BS antennas $M = 5$.

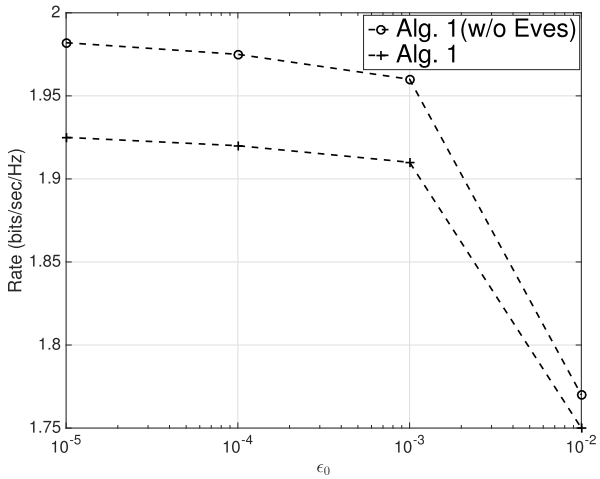

Fig. 6. Robust secrecy rate (with eavesdroppers) and normal rate (without eavesdroppers) versus different levels of channel uncertainty ϵ_0 for fixed energy harvesting threshold $e^{\min} = -20$ dBm and number of BS antennas $M = 5$.

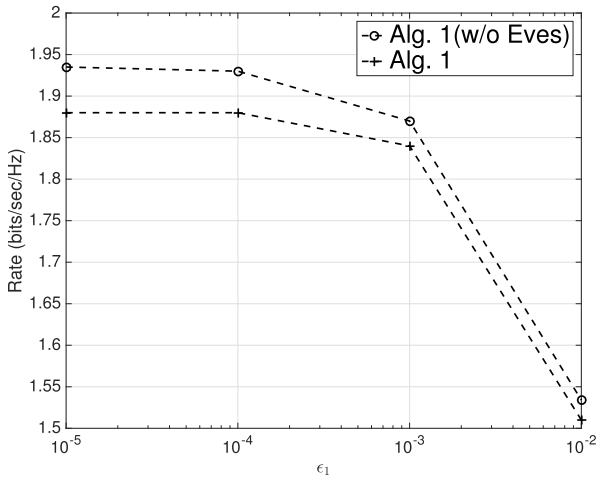

Fig. 7. Robust secrecy rate (with eavesdroppers) and normal rate (without eavesdroppers) versus different levels of channel uncertainty ϵ_1 for fixed energy harvesting threshold $e^{\min} = -20$ dBm and number of BS antennas $M = 5$.

uncertainties, and close to the case that assumes perfect channel estimation. However, the performance gap increases as the number of BS antennas increases as can be seen from Fig. 4. This is expected because increasing the number of BS antennas, say from $M = 4$ to $M = 5$, increases the channel uncertainty in an additional $KN = 12$ channel co-efficients. Moreover, we observe that the optimized rate obtained by the proposed Algorithm 1 is quite close to that achieved by the modified algorithm, which assumes the absence of eavesdroppers in Algorithm 1. Fig. 4 plots the rate for different numbers of BS antennas $M \in \{4, 5, 6\}$ with fixed EH threshold $e^{\min} = -20$ dBm, while Fig. 5 plots the rate for varying values of EH targets $e^{\min} \in \{-25, -20, \ldots, 0\}$ dBm with fixed number of antennas at the BS $M = 5$. In Fig. 4, we observe an almost linear increase in the achievable rate as the number of BS antennas increases. In Fig. 5, we observe a decrease in the achievable rate with an increase in the EH targets. This is because higher EH targets require more power from the BSs to perform energy harvesting, which results in a decrease in the available power for information decoding, thus decreasing the achievable information rate. Overall, Figs. 4 and 5 indicate the robustness of our proposed Algorithm 1.

Fig. 6 plots the worst secrecy and normal rates (in the absence of eavesdroppers) versus the level of channel uncertainty in the neighboring users' channels and the eavesdroppers' channels $\epsilon_0 = \{10^{-5}, \ldots, 10^{-2}\}$ for fixed $\epsilon_1 = 10^{-3}$, while Fig. 7 plots such rates versus the level of channel uncertainty in the serving BS users' channels $\epsilon_0 = \{10^{-5}, \ldots, 10^{-2}\}$ for fixed $\epsilon_0 = 0.005$. We set the energy harvesting threshold $e^{\min} = -20$ dBm and number of BS antennas $M = 5$. We can observe from Figs. 6 and 7 that the optimized rate is almost unaffected for low channel uncertainties $\{10^{-5}, \ldots, 10^{-3}\}$, and is slightly reduced if channel uncertainty is increased to the level of 10^{-2}. This confirms the robustness of the solution of Algorithm 1. Even for a wide range of values of channel uncertainty ϵ_0, the

TABLE I

COMPLEXITY ANALYSIS FOR THE PROPOSED TS-BASED ALG. 1 AND PS-BASED ALGORITHM IN [18] FOR GENERAL M, N, K, AND SPECIFIC $M = 4$, $N = 4$, $K = 3$ CASES

Algorithms	avg. # iter	scalar variables	linear constraints	quadratic constraints
Algorithm 1	22.5	$MK(N+N_1)+1=73$	$3KN+KN_1+(K+1)=46$	$4KN+2KN_1+1=61$
PS Algorithm [18]	16	$MK(N+1)+KN_1=66$	$K+1=4$	$KN+3KN_1=30$

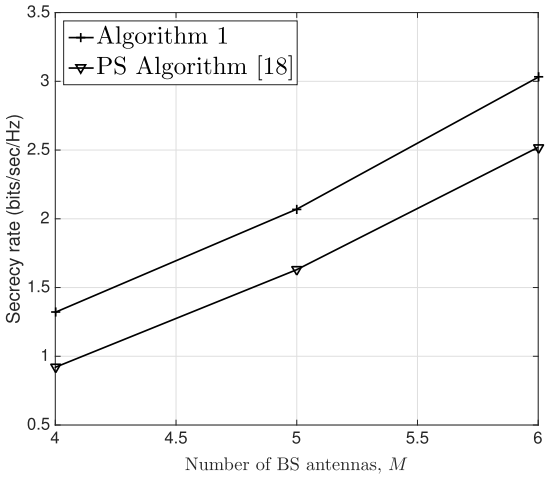

Fig. 8. Comparison of the proposed secrecy rate TS-based Algorithm 1 with the existing PS-based algorithm [18] for fixed energy harvesting threshold $e^{\min} = -20$ dBm and perfect channel estimation $\epsilon_0 = \epsilon_1 = 0$.

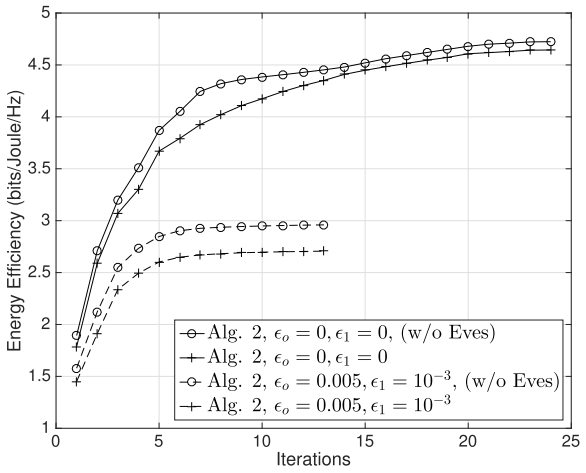

Fig. 9. Convergence of Algorithm 2 for $M = 5$ and $e^{\min} = -20$ dBm.

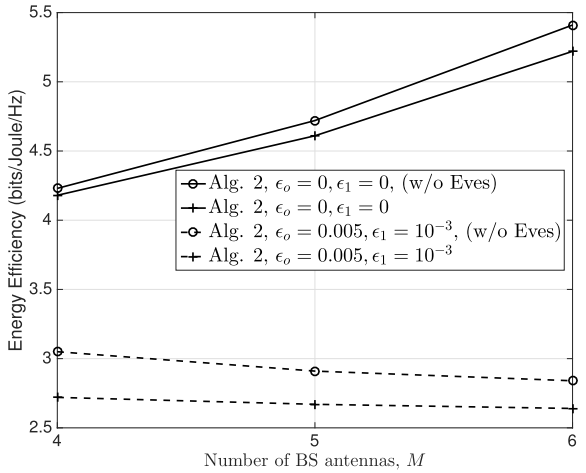

Fig. 10. Robust secrecy energy efficiency and normal energy efficiency in the presence and absence of eavesdroppers, respectively, for varying numbers of antennas M with fixed EH threshold $e^{\min} = -20$ dBm.

optimized secrecy rate attained by Algorithm 1 is quite close to that achieved by the modified algorithm, which assumes the absence of eavesdroppers in Algorithm 1.

Fig. 8 compares the secrecy rate performance of the proposed transmit TS-based system with that of the PS-based system [18] under perfect channel state information ($\epsilon_0 = 0$, $\epsilon_1 = 0$). For the PS-based receiver in [18], we set the ID circuit noise variance σ_c^2 to be -90 dBm and the antenna noise variance $\sigma_a^2 = -90$ dBm. Thus, for fair comparison in Fig. 8, we add σ_c^2 to σ_a^2, i.e., $\sigma_a^2 = -87$ dBm, for plotting the results for our proposed TS-based Algorithm 1. Fig. 8 plots the worst secrecy rate versus the number of antennas M for fixed energy harvesting threshold $e^{\min} = -20$ dBm. We can clearly observe a gain of around 0.5 bits/sec/Hz in the achieved secrecy rate of Algorithm 1 compared to that of the algorithm in [18]. Note that the proposed TS-based system not only enjoys a performance gain, but also is simple to implement. The average numbers of iterations required for convergence are almost the same for both Algorithm 1 and the algorithm in [18].

The computational complexity of the proposed Algorithm 1 is $O(i_{\mathrm{A1}}(MK(N+N_1)+1)^3(7KN+(K+2)+3KN_1))$ [52]. Here, $i_{\mathrm{A1}} = 22.5$ is the average number of times that (41) is solved by Algorithm 1. Table I shows the average number of iterations, scalar variables, and linear and quadratic constraints that must be solved per iteration by the proposed Algorithm 1 and the PS-based algorithm in [18]. We can observe that though the PS-based algorithm in [18] requires the solution of fewer quadratic and linear constraints, it is not practically easy to implement a variable range power splitter. Thus, the proposed TS-based Algorithm 1 provides a more practical solution to secure and robust beamforming.

Finally, the performance of our proposed SEE Algorithm 2 is evaluated. Fig. 9 shows the convergence of proposed Algorithm 2 for $M = 5$ antennas at the BS and energy harvesting threshold $e^{\min} = -20$ dBm. We can see that for some fixed channel, whether we assume perfect channel estimation $\epsilon_0 = 0$, $\epsilon_1 = 0$, or assume some channel uncertainty $\epsilon_0 = 0.005$, $\epsilon_0 = 10^{-3}$, Algorithm 2 converges within $20 - 25$ iterations. On average, Algorithm 2 requires approximately 18.5 iterations for convergence.

Figs. 10 and 11 plot the secrecy energy efficiency and normal energy efficiency (in the absence of eavesdroppers)

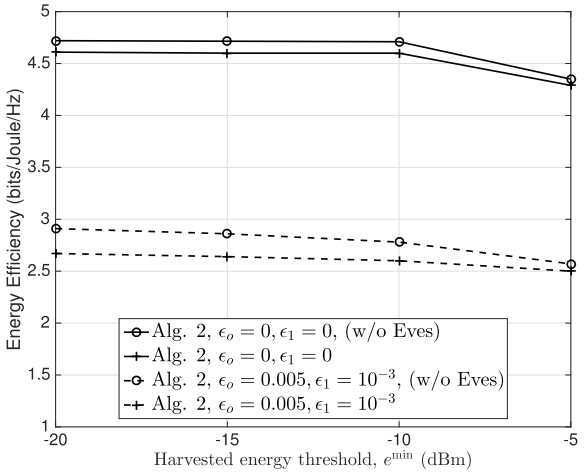

Fig. 11. Robust secrecy energy efficiency and normal energy efficiency in the presence and absence of eavesdroppers, respectively, for different values of the EH threshold $e^{\min}$ with fixed number of BS antennas $M = 5$.

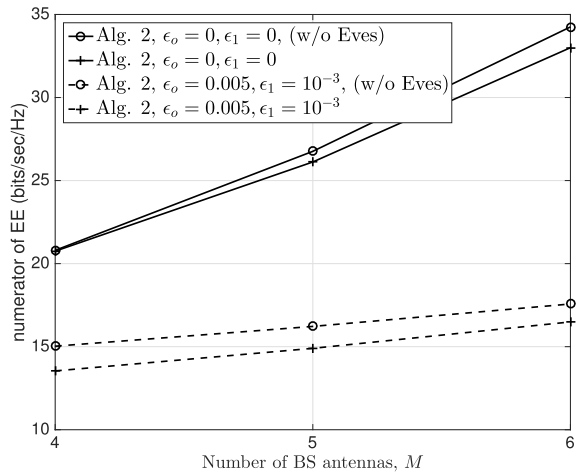

Fig. 12. Numerator of energy efficiency (sum-rate of the worst cell) in the presence of eavesdroppers for varying numbers of antennas M with fixed EH threshold $e^{\min} = -20$ dBm.

for both perfect channel estimation $\epsilon_0 = 0$, $\epsilon_1 = 0$, and with the presence of channel uncertainty $\epsilon_0 = 0.005$, $\epsilon_1 = 10^{-3}$. Here, the achievable SEE for Algorithm 2 is compared with the normal EE assuming no eavesdroppers, that is obtained by solving the optimization problem (45) with $f_{k,n}^2(\mathbf{x}, \eta) \equiv 0$. The dashed curves in Figs. 10 and 11 correspond to the presence of channel uncertainties $\epsilon_0 = 0.005$, $\epsilon_1 = 10^{-3}$, while the solid curves correspond to the absence of channel uncertainty $\epsilon_0 = \epsilon_1 = 0$. We can observe from Figs. 10 and 11 that the optimized EE attained by the proposed Algorithm 2 is quite close to that achieved by the modified algorithm, which assumes absence of eavesdroppers in Algorithm 2. Finally, we observe from Fig. 10 that for perfect channel estimation, the optimized EE increases as the number of antennas increases, as per expectation; however, in the presence of channel uncertainties, the EE decreases with an increase in the number of antennas. In order to investigate this, we have separated out the numerator and denominator of the EE separately in the next two figures.

In Figs. 12 and 13, we plot the numerator and denominator of the EE expression, (45a), respectively, where the numerator corresponds to the sum-rate of the worst cell and the

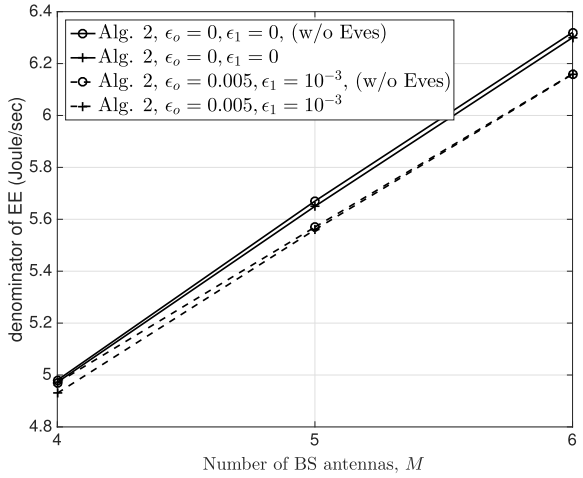

Fig. 13. Denominator of energy efficiency (total power of the worst cell's BS) in the presence of eavesdroppers for varying numbers of antennas M with fixed EH threshold $e^{\min} = -20$ dBm.

denominator corresponds to the total power, $\frac{1}{\xi} g_k(\mathbf{x}_k, \eta) + MP_A + P_c$, of the worst cell's BS. First, we can observe from Fig. 13 that the denominator of the EE expression increases with an increase in the number of BS antennas. This is because an increase in the number of BS antennas increases the non-transmission power MP_A in the denominator of the EE expression, (45a). Next, we can observe from Fig. 12 that though the numerator of the EE expression also increases with an increase in the number of BS antennas, the numerator increases rapidly for the prefect channel estimation case (solid lines) when compared to its slow increase in the presence of channel uncertainties (dashed lines). This results in a slight decrease in the EE with an increase in the number of antennas in the presence of estimation errors, as shown in Fig. 10.

VI. Conclusions

Considering a transmit TS approach to wireless energy harvesting and information decoding in a dense multi-cell network, we have proposed robust secrecy rate and secrecy energy efficiency maximization algorithms in the presence of multi-antenna eavesdroppers and channel estimation errors. Our robust optimization algorithm jointly designs transmit energy and information beamformers at the BSs and the transmit TS ratio with the objective of maximizing the worst-case user secrecy rate under BS transmit power and UE minimum harvested energy constraints. The problem is very challenging due to its non-convex objective and numerous non-convex constraints. We have solved it by a new robust path-following algorithm, which involves one simple convex quadratic program at each iteration. We have also extended our algorithm to solve the worst cell secrecy EE maximization problem under secrecy rate quality-of-service constraints, which adds further complexity due to additional optimization variables in the denominator of the secrecy rate function. Our numerical results confirm the merits of the proposed algorithms as their performance is quite close to that of the case where there are no eavesdroppers. Moreover, the proposed algorithm not only outperforms the existing algorithm that uses a PS based receiver but also the proposed transmit TS based model is implementation-wise simpler than the PS-based system. Note that we have not considered the worst case scenario in which

eavesdroppers know the time switching ratio. Secrecy rate maximization under this situation can be based on the use of power splitting instead of time switching as proposed in our previous work [18], whereas the use of the techniques in the current work in this situation is an interesting topic for further work.

APPENDIX
PROOF OF THEOREM 1

We first prove (30) by using the following inequality for all $x > 0$, $\bar{x} > 0$, $t > 0$ and $\bar{t} > 0$:

$$\begin{aligned}\frac{\ln(1+1/x)}{t} &\geq f(\bar{x},\bar{t}) + \langle \nabla f(\bar{x},\bar{t}), (x,t) - (\bar{x},\bar{t})\rangle \\ &= 2\frac{\ln(1+1/\bar{x})}{\bar{t}} + \frac{1}{\bar{t}(\bar{x}+1)} \\ &\quad - \frac{x}{(\bar{x}+1)\bar{x}\bar{t}} - \frac{\ln(1+1/\bar{x})}{\bar{t}^2}t. \end{aligned} \tag{A.1}$$

which follows from the convexity of the function $\frac{\ln(1+1/x)}{t}$.

By subsituting $1/x \to x$ and $1/\bar{x} \to \bar{x}$ in (A.1), we have

$$\frac{\ln(1+x)}{t} \geq a - \frac{b}{x} - ct, \tag{A.2}$$

where $a = 2\frac{\ln(1+\bar{x})}{\bar{t}} + \frac{\bar{x}}{\bar{t}(\bar{x}+1)} > 0, b = \frac{\bar{x}^2}{\bar{t}(\bar{x}+1)} > 0$, $c = \frac{\ln(1+\bar{x})}{\bar{t}^2} > 0$. From this, it follows that,

$$\begin{aligned}&\frac{1}{\mu}\ln\left(1 + \frac{\left(\Re\{\mathbf{h}_{k,k,n}^H \mathbf{x}_{k,n}^I\}\right)^2 - \epsilon_{k,k,n}\|\mathbf{x}_{k,n}^I\|^2}{\varphi_{k,n}(\mathbf{x}^I)}\right) \\ &\geq a^{(\ell)} - b^{(\ell)}\frac{\varphi_{k,n}(\mathbf{x}^I)}{\left(\Re\left\{\mathbf{h}_{k,k,n}^H \mathbf{x}_{k,n}^I\right\}\right)^2 - \epsilon_{k,k,n}\|\mathbf{x}_{k,n}^I\|^2} - c^{(\ell)}\mu, \end{aligned} \tag{A.3}$$

where $a^{(\ell)}$, $b^{(\ell)}$, $c^{(\ell)}$, and $d^{(\ell)}$ are defined in (32). Now, using $(\Re\{\mathbf{h}_{k,k,n}^H \mathbf{x}_{k,n}^I\})^2 \geq \psi_{k,n}(\mathbf{x}_{k,n}^I)$ with $\psi_{k,n}(\mathbf{x}_{k,n}^I) \geq 0$ defined in (33), together with (A.3) leads to

$$\begin{aligned}&\frac{1}{\mu}\ln\left(1 + \frac{\left(\Re\left\{\mathbf{h}_{k,k,n}^H \mathbf{x}_{k,n}^I\right\}\right)^2 - \epsilon_{k,k,n}\|\mathbf{x}_{k,n}^I\|^2}{\varphi_{k,n}(\mathbf{x}^I)}\right) \\ &\geq a^{(\ell)} - b^{(\ell)}\frac{\varphi_{k,n}(\mathbf{x}^I)}{\nu_{k,n}(\mathbf{x}_{k,n}^I)} - c^{(\ell)}\mu \\ &\triangleq \bar{f}_{k,n}^{1,(\ell)}(\mathbf{x}^I, \mu) \end{aligned} \tag{A.4}$$

for $0 \leq \nu_{k,n}(\mathbf{x}_{k,n}^I) \leq \psi_{k,n}(\mathbf{x}_{k,n}^I) - \epsilon_0||\mathbf{x}_{k,n}^I||^2$, $\forall k \in \mathcal{K}, n \in \mathcal{N}_k$. The function $\bar{f}_{k,n}^{1,(\ell)}(\mathbf{x}^I, \mu)$ is concave on (31).

Next, (34) follows from the following inequality:

$$\ln(1+t) \leq \ln(1+t') + (t-t')/(1+t') \quad \forall t \geq 0, \ t' \geq 0,$$

which is a consequence of the concavity of the function $\ln(1+t)$.

Now, it remains to prove (21). By substituting $\bar{q}_{k,n}(\mathbf{x}, \mu)$, defined in (21), into the constraint (36), we have

$$\begin{aligned}&\frac{\sqrt{\beta_{k,n}}}{\mu-1} + \frac{1}{\mu-1}\left(\sum_{\bar{n}\in\mathcal{N}_k\setminus\{n\}} \epsilon_{k,k}\|\mathbf{x}_{k,\bar{n}}^I\|^2 \right. \\ &\qquad \left. + \sum_{\bar{k}\in\mathcal{K}\setminus\{k\}}\sum_{\bar{n}\in\mathcal{N}_{\bar{k}}} \epsilon_{\bar{k},k}\|\mathbf{x}_{\bar{k},\bar{n}}^I\|^2\right) + \sum_{\bar{k}\in\mathcal{K}}\sum_{\bar{n}\in\mathcal{N}_{1,k}} \epsilon_{\bar{k},k}\|\mathbf{x}_{\bar{k},\bar{n}}^E\|^2 \\ &\leq \sum_{\bar{k}\in\mathcal{K}}\sum_{\bar{n}\in\mathcal{N}_{1,k}} \|\boldsymbol{\mathcal{H}}_{\bar{k},k}^H \mathbf{x}_{\bar{k},\bar{n}}^E\|^2 \\ &\qquad + \frac{1}{\mu-1}\left(\sum_{\bar{n}\in\mathcal{N}_k\setminus\{n\}} \|\boldsymbol{\mathcal{H}}_{k,k}^H \mathbf{x}_{k,\bar{n}}^I\|^2 \right. \\ &\qquad \left. + \sum_{\bar{k}\in\mathcal{K}\setminus\{k\}}\sum_{\bar{n}\in\mathcal{N}_{\bar{k}}} \|\boldsymbol{\mathcal{H}}_{\bar{k},k}^H \mathbf{x}_{\bar{k},\bar{n}}^I\|^2\right) + (1 + \frac{1}{\mu-1})N_{\text{ev}}\sigma_a^2, \end{aligned} \tag{A.5}$$

where the right hand side of (A.5) is convex and can be linearized for inner approximation by using [49]

$$\frac{\|\mathbf{x}\|^2}{y} \geq \frac{2\Re\left\{(\mathbf{x}^{(\ell)})^H \mathbf{x}\right\}}{y^{(\ell)}} - \frac{\|\mathbf{x}^{(\ell)}\|^2 y}{\left(y^{(\ell)}\right)^2}, \tag{A.6}$$

$$\forall \mathbf{x} \in \mathbb{C}^N, \quad \mathbf{x}^{(\ell)} \in \mathbb{C}^N, \ y > 0, \ y^{(\ell)} > 0,$$

$$\|\mathbf{x}\|^2 \geq 2\Re\left\{(\mathbf{x}^{(\ell)})^H \mathbf{x}\right\} - \|\mathbf{x}^{(\ell)}\|^2, \tag{A.7}$$

$$\forall \mathbf{x} \in \mathbb{C}^N, \quad \mathbf{x}^{(\ell)} \in \mathbb{C}^N \tag{A.8}$$

and

$$\frac{1}{\mu-1} \geq \frac{2}{\mu^{(\ell)}-1} - \frac{\mu-1}{(\mu^{(\ell)}-1)^2}. \tag{A.9}$$

The first term on the left hand side of (A.5) is non-convex, which is convexified by using the fact that $\sqrt{xy}$ is concave in x and y, i.e., $\sqrt{xy} \leq \frac{\sqrt{s^{(\ell)}}y}{2\sqrt{y^{(\ell)}}} + \frac{\sqrt{y^{(\ell)}}x}{2\sqrt{s^{(\ell)}}}$. Thus, $\frac{\sqrt{\beta_{k,n}}}{\mu-1}$ can be approximated as

$$\frac{\sqrt{\beta_{k,n}}}{\mu-1} \leq \frac{1}{2}\left(\frac{\beta_{k,n}}{\sqrt{\beta_{k,n}^{(\ell)}}(\mu^{(\ell)}-1)} + \frac{\sqrt{\beta_{k,n}^{(\ell)}}(\mu^{(\ell)}-1)}{(\mu-1)^2}\right). \tag{A.10}$$

Thus, using (A.6), (A.7), (A.9), and (A.10) in (A.5), we obtain the approximation (37).

REFERENCES

[1] X. Lu, P. Wang, D. Niyato, D. I. Kim, and Z. Han, "Wireless networks with RF energy harvesting: A contemporary survey," *IEEE Commun. Surveys Tuts.*, vol. 17, no. 2, pp. 757–789, 2nd Quart., 2015.

[2] Z. Ding, S. M. Perlaza, I. Esnaola, and H. V. Poor, "Power allocation strategies in energy harvesting wireless cooperative networks," *IEEE Trans. Wireless Commun.*, vol. 13, no. 2, pp. 846–860, Feb. 2014.

[3] I. Krikidis, S. Timotheou, S. Nikolaou, G. Zheng, D. W. K. Ng, and R. Schober, "Simultaneous wireless information and power transfer in modern communication systems," *IEEE Commun. Mag.*, vol. 52, no. 11, pp. 104–110, Nov. 2014.

[4] J. Xu, L. Liu, and R. Zhang, "Multiuser MISO beamforming for simultaneous wireless information and power transfer," *IEEE Trans. Signal Process.*, vol. 62, no. 18, pp. 4798–4810, Sep. 2014.

[5] Y. Zeng and R. Zhang, "Optimized training design for wireless energy transfer," *IEEE Trans. Commun.*, vol. 63, no. 2, pp. 536–550, Feb. 2015.

[6] R. Zhang and C. K. Ho, "MIMO broadcasting for simultaneous wireless information and power transfer," *IEEE Trans. Wireless Commun.*, vol. 12, no. 5, pp. 1989–2001, May 2013.

[7] A. A. Nasir, X. Zhou, S. Durrani, and R. A. Kennedy, "Relaying protocols for wireless energy harvesting and information processing," *IEEE Trans. Wireless Commun.*, vol. 12, no. 7, pp. 3622–3636, Jul. 2013.

[8] A. A. Nasir, H. D. Tuan, D. T. Ngo, T. Q. Duong, and H. V. Poor, "Beamforming design for wireless information and power transfer systems: Receive power-splitting versus transmit time-switching," *IEEE Trans. Commun.*, vol. 65, no. 2, pp. 876–889, Feb. 2017.

[9] A. G. Fragkiadakis, E. Z. Tragos, and I. G. Askoxylakis, "A survey on security threats and detection techniques in cognitive radio networks," *IEEE Commun. Surveys Tuts.*, vol. 15, no. 1, pp. 428–445, 1st Quart., 2013.

[10] T. M. Hoang, T. Q. Duong, H. A. Suraweera, C. Tellambura, and H. V. Poor, "Cooperative beamforming and user selection for improving the security of relay-aided systems," *IEEE Trans. Commun.*, vol. 63, no. 12, pp. 5039–5051, Dec. 2015.

[11] H. V. Poor, "Information and inference in the wireless physical layer," *IEEE Wireless Commun.*, vol. 19, no. 1, pp. 40–47, Feb. 2012.

[12] R. Liu and W. Trappe, Eds., *Securing Wireless Communications at the Physical Layer*. New York, NY, USA: Springer-Verlag, 2010.

[13] M. Bloch and J. Barros, *Physical-Layer Security*. Cambridge, U.K.: Cambridge Univ. Press, 2011.

[14] A. Mukherjee and A. L. Swindlehurst, "Robust beamforming for security in MIMO wiretap channels with imperfect CSI," *IEEE Trans. Signal Process.*, vol. 59, no. 1, pp. 351–361, Jan. 2011.

[15] Q. Li and W.-K. Ma, "Spatially selective artificial-noise aided transmit optimization for MISO multi-eves secrecy rate maximization," *IEEE Trans. Signal Process.*, vol. 61, no. 10, pp. 2704–2717, May 2013.

[16] P. Zhao, M. Zhang, H. Yu, H. Luo, and W. Chen, "Robust beamforming design for sum secrecy rate optimization in MU-MISO networks," *IEEE Trans. Inf. Forensics Security*, vol. 10, no. 9, pp. 1812–1823, Sep. 2015.

[17] Z. Chu, Z. Zhu, M. Johnston, and S. Y. Le Goff, "Simultaneous wireless information power transfer for MISO secrecy channel," *IEEE Trans. Veh. Technol.*, vol. 65, no. 9, pp. 6913–6925, Sep. 2016.

[18] A. A. Nasir, H. D. Tuan, T. Q. Duong, and H. V. Poor, "Secrecy rate beamforming for multicell networks with information and energy harvesting," *IEEE Trans. Signal Process.*, vol. 65, no. 3, pp. 677–689, Feb. 2017.

[19] Q. Zhang, X. Huang, Q. Li, and J. Qin, "Cooperative jamming aided robust secure transmission for wireless information and power transfer in MISO channels," *IEEE Trans. Commun.*, vol. 63, no. 3, pp. 906–915, Mar. 2015.

[20] Z. Zhu, Z. Chu, Z. Wang, and I. Lee, "Outage constrained robust beamforming for secure broadcasting systems with energy harvesting," *IEEE Trans. Wireless Commun.*, vol. 15, no. 11, pp. 7610–7620, Nov. 2016.

[21] R. Feng, Q. Li, Q. Zhang, and J. Qin, "Robust secure transmission in MISO simultaneous wireless information and power transfer system," *IEEE Trans. Veh. Technol.*, vol. 64, no. 1, pp. 400–405, Jan. 2015.

[22] H. Zhang, Y. Huang, C. Li, and L. Yang, "Secure beamforming design for SWIPT in MISO broadcast channel with confidential messages and external eavesdroppers," *IEEE Trans. Wireless Commun.*, vol. 15, no. 11, pp. 7807–7819, Nov. 2016.

[23] A. H. Phan, H. D. Tuan, H. H. Kha, and D. T. Ngo, "Nonsmooth optimization for efficient beamforming in cognitive radio multicast transmission," *IEEE Trans. Signal Process.*, vol. 60, no. 6, pp. 2941–2951, Jun. 2012.

[24] R. L. G. Cavalcante, S. Stanczak, M. Schubert, A. Eisenblaetter, and U. Tuerke, "Toward energy-efficient 5G wireless communications technologies: Tools for decoupling the scaling of networks from the growth of operating power," *IEEE Signal Process. Mag.*, vol. 31, no. 6, pp. 24–34, Nov. 2014.

[25] C.-L. I, C. Rowell, S. Han, Z. Xu, G. Li, and Z. Pan, "Toward green and soft: A 5G perspective," *IEEE Commun. Mag.*, vol. 52, no. 2, pp. 66–73, Feb. 2014.

[26] S. Buzzi, C.-L. I, T. E. Klein, H. V. Poor, C. Yang, and A. Zappone, "A survey of energy-efficient techniques for 5G networks and challenges ahead," *IEEE J. Sel. Areas Commun.*, vol. 34, no. 4, pp. 697–709, Apr. 2016.

[27] D. W. K. Ng, E. S. Lo, and R. Schober, "Energy-efficient resource allocation for secure OFDMA systems," *IEEE Trans. Veh. Technol.*, vol. 61, no. 6, pp. 2572–2585, Jul. 2012.

[28] X. Chen and L. Lei, "Energy-efficient optimization for physical layer security in multi-antenna downlink networks with QoS guarantee," *IEEE Commun. Lett.*, vol. 17, no. 4, pp. 637–640, Apr. 2013.

[29] A. Zappone, P. H. Lin, and E. Jorswieck, "Energy efficiency of confidential multi-antenna systems with artificial noise and statistical CSI," *IEEE J. Sel. Topics Signal Process.*, vol. 10, no. 8, pp. 1462–1477, Dec. 2016.

[30] W. Dinkelbach, "On nonlinear fractional programming," *Manage. Sci.*, vol. 13, no. 7, pp. 492–498, Mar. 1967. [Online]. Available: http://www.jstor.org/stable/2627691

[31] A. Zappone and E. Jorswieck, "Energy efficiency in wireless networks via fractional programming theory," *Found. Trends Commun. Inf. Theory*, vol. 11, no. 3–4, pp. 185–396, 2015.

[32] A. Zappone, L. Sanguinetti, G. Bacci, E. Jorswieck, and M. Debbah, "Energy-efficient power control: A look at 5G wireless technologies," *IEEE Trans. Signal Process.*, vol. 64, no. 4, pp. 1668–1683, Apr. 2016.

[33] N. Zhao, F. R. Yu, and H. Sun, "Adaptive energy-efficient power allocation in green interference-alignment-based wireless networks," *IEEE Trans. Veh. Technol.*, vol. 64, no. 9, pp. 4268–4281, Sep. 2015.

[34] T. T. Vu, H. H. Kha, and H. D. Tuan, "Transceiver design for optimizing the energy efficiency in multiuser MIMO channels," *IEEE Commun. Lett.*, vol. 20, no. 8, pp. 1507–1510, Aug. 2016.

[35] S. Guo, C. He, and Y. Yang, "ResAll: Energy efficiency maximization for wireless energy harvesting sensor networks," in *Proc. IEEE SECON*, Jun. 2015, pp. 64–72.

[36] Q.-D. Vu, L.-N. Tran, R. Farrell, and E.-K. Hong, "An efficiency maximization design for SWIPT," *IEEE Signal Process. Lett.*, vol. 22, no. 12, pp. 2189–2193, Dec. 2015.

[37] S. Leng, D. W. K. Ng, N. Zlatanov, and R. Schober, "Multi-objective beamforming for energy-efficient SWIPT systems," in *Proc. IEEE ICNC*, Feb. 2016, pp. 1–7.

[38] B. Clerckx and E. Bayguzina, "Waveform design for wireless power transfer," *IEEE Trans. Signal Process.*, vol. 64, no. 23, pp. 6313–6328, Dec. 2016.

[39] B. Clerckx. (May 2017). "Wireless information and power transfer: Nonlinearity, waveform design and rate-energy tradeoff." [Online]. Available: https://arxiv.org/abs/1607.05602

[40] Y. Zeng, B. Clerckx, and R. Zhang, "Communications and signals design for wireless power transmission," *IEEE Trans. Commun.*, vol. 65, no. 5, pp. 2264–2290, May 2017.

[41] J. Huang and A. L. Swindlehurst, "Robust secure transmission in MISO channels based on worst-case optimization," *IEEE Trans. Signal Process.*, vol. 60, no. 4, pp. 1696–1707, Apr. 2012.

[42] U. Rashid, H. D. Tuan, and H. H. Nguyen, "Relay beamforming designs in multi-user wireless relay networks based on throughput maximin optimization," *IEEE Trans. Commun.*, vol. 51, no. 5, pp. 1739–1749, May 2013.

[43] L. Dong, Z. Han, A. P. Petropulu, and H. V. Poor, "Improving wireless physical layer security via cooperating relays," *IEEE Trans. Signal Process.*, vol. 58, no. 3, pp. 1875–1888, Mar. 2010.

[44] J. Li, A. P. Petropulu, and S. Weber, "On cooperative relaying schemes for wireless physical layer security," *IEEE Trans. Signal Process.*, vol. 59, no. 10, pp. 4985–4997, Oct. 2011.

[45] Z. Ding, K. K. Leung, D. L. Goeckel, and D. Towsley, "On the application of cooperative transmission to secrecy communications," *IEEE J. Sel. Areas Commun.*, vol. 30, no. 2, pp. 359–368, Feb. 2012.

[46] Y. Liang, G. Kramer, H. V. Poor, and S. Shamai (Shitz), "Compound wire-tap channels," *EURASIP J. Wireless Commun. Netw.*, vol. 2009, no. 1, Oct. 2009, Art. no. 142374.

[47] H. Tuy, *Convex Analysis and Global Optimization*, 2nd ed. Springer, 2016.

[48] A. Wiesel, Y. C. Eldar, and S. Shamai (Shitz), "Linear precoding via conic optimization for fixed MIMO receivers," *IEEE Trans. Signal Process.*, vol. 54, no. 1, pp. 161–176, Jan. 2006.

[49] A. A. Nasir, H. D. Tuan, D. T. Ngo, S. Durrani, and D. I. Kim, "Path-following algorithms for beamforming and signal splitting in RF energy harvesting networks," *IEEE Commun. Lett.*, vol. 20, no. 8, pp. 1687–1690, Aug. 2016.

[50] O. Onireti, A. Imran, M. A. Imran, and R. Tafazolli, "Energy efficient inter-frequency small cell discovery in heterogeneous networks," in *Proc. IEEE ICC*, Jun. 2015, pp. 13–18.

[51] G. Auer *et al.*, "D2.3: Energy efficiency analysis of the reference systems, areas of improvements and target breakdown," *EARTH: Energy Aware Radio Netw. Technol.* [Online]. Available: https://bscw.ict-earth.eu/pub/bscw.cgi/d71252/ EARTH_WP2_D2.3_v2.pdf

[52] D. Peaucelle, D. Henrion, and Y. Labit. (2002). *User's Guide for SeDuMi Interface 1.03*. [Online]. Available: http://homepages.laas.fr/peaucell/software/sdmguide.pdf

Ali Arshad Nasir (S'09–M'13) received the Ph.D. degree in telecommunications engineering from Australian National University (ANU), Australia, in 2013. He was a Research Fellow with ANU from 2012 to 2015. He held an assistant professor position with the School of Electrical Engineering and Computer Science, National University of Sciences and Technology, Pakistan, from 2015 to 2016. He is currently an Assistant Professor with the Department of Electrical Engineering, King Fahd University of Petroleum and Minerals, Dhahran, Kingdom of Saudi Arabia. His research interests are in the area of signal processing in wireless communication systems. He is currently an Associate Editor of the IEEE CANADIAN JOURNAL OF ELECTRICAL AND COMPUTER ENGINEERING.

Hoang Duong Tuan received the Diploma (Hons.) and Ph.D. degrees in applied mathematics from Odessa State University, Ukraine, in 1987 and 1991, respectively. He spent nine academic years in Japan as an Assistant Professor with the Department of Electronic-Mechanical Engineering, Nagoya University, from 1994 to 1999, and then as an Associate Professor with the Department of Electrical and Computer Engineering, Toyota Technological Institute, Nagoya, from 1999 to 2003. He was a Professor with the School of Electrical Engineering and Telecommunications, University of New South Wales, from 2003 to 2011. He is currently a Professor with the School of Electrical and Data Engineering, University of Technology Sydney. He has been involved in research in the areas of optimization, control, signal processing, wireless communication, and biomedical engineering for over 20 years.

Trung Q. Duong (S'05–M'12–SM'13) received the Ph.D. degree in telecommunications systems from the Blekinge Institute of Technology, Sweden, in 2012. Since 2013, he has been with Queen's University Belfast, U.K., as a Lecturer (Assistant Professor). His current research interests include small-cell networks, physical layer security, energy-harvesting communications, and cognitive relay networks. He has authored or co-authored over 260 technical papers published in scientific journals (142 articles) and presented at international conferences (121 papers).

Dr. Duong currently serves as an Editor of the IEEE TRANSACTIONS ON WIRELESS COMMUNICATIONS, the IEEE TRANSACTIONS ON COMMUNICATIONS, the *IET Communications*, and a Senior Editor of the IEEE COMMUNICATIONS LETTERS. He was a recipient of the Best Paper Award at the IEEE Vehicular Technology Conference in 2013, the IEEE International Conference on Communications 2014, and the IEEE Global Communications Conference 2016. He is a recipient of a prestigious Royal Academy of Engineering Research Fellowship (2016–2021).

H. Vincent Poor (S'72–M'77–SM'82–F'87) received the Ph.D. degree in EECS from Princeton University in 1977. From 1977 to 1990, he was on the faculty of the University of Illinois at Urbana–Champaign. Since 1990, he has been on the faculty at Princeton, where he is currently the Michael Henry Strater University Professor of Electrical Engineering. During 2006 to 2016, he served as the Dean of the Princeton's School of Engineering and Applied Science. His research interests are in the areas of information theory and signal processing, and their applications in wireless networks and related fields such as smart grid and social networks. Among his publications in these areas is the book *Information Theoretic Security and Privacy of Information Systems* (Cambridge University Press, 2017).

Dr. Poor is a member of the National Academy of Engineering and the National Academy of Sciences, and is a foreign member of the Royal Society. He is also a fellow of the American Academy of Arts and Sciences, the National Academy of Inventors, and other national and international academies. He received the Marconi and Armstrong Awards of the IEEE Communications Society in 2007 and 2009, respectively. Recent recognition of his work includes the 2016 John Fritz Medal, the 2017 IEEE Alexander Graham Bell Medal, Honorary Professorships at Peking University and Tsinghua University, both conferred in 2017, and a D.Sc. *honoris causa* from Syracuse University received in 2017.